site, but a microenvironment that supports the proliferation and differentiation of those cells is also needed [28,29]. In anticipation of favorable articular cartilage repair in the osteochondral defect model, reparative cells must be provided with an environment to acquire the properties of natural articular cartilage. We recently constructed a 3-D, scaffold-free, tissue-engineered cartilage [24] and transplanted this cartilage in only the superficial layer region of the osteochondral defects as an initiator of cartilage differentiation in reparative cells [23] and achieved good restoration effects in the long term [29]. We confirmed that in the early stage of transplantation, a good restoration effect of articular cartilage is seen with reparative cells derived from marrow that acquire antiangiogenic properties [23]. We therefore hypothesized that good cartilage repair may be achieved by inhibiting the bioactivity of vascular endothelial growth factor (VEGF) in the osteochondral defect. A recent investigation examined the effect of treatment with anti-VEGF humanized monoclonal antibody (bevacizumab), which was developed as a treatment for malignant tumors [30]. Bevacizumab binds to VEGF secreted by angiogenic tumors and thereby inhibits VEGF binding to the VEGF receptor in vascular endothelial cells, reportedly restraining cancer growth by inhibiting angiogenesis [31,32].

The objective of this study is to investigate the efficacy of repair in an osteochondral defect model of the rabbit knee joint following administration of bevacizumab, a humanized monoclonal anti-VEGF antibody, without using cultured cells or artificial scaffolds.

Materials and methods

Animal experiments were approved by the ethics review board of Tokai University and were performed in accordance with the guidelines on animal use of Tokai University.

Repair of the osteochondral defect

Twenty Japanese white rabbits (female, 16-18 weeks old, weighing approximately 3 kg) were used in this study. The rabbits were anesthetized by exposure to sevoflurane and O_2 gas. After receiving a medial parapatellar incision to both legs, each patella was dislocated laterally and an osteochondral defect (diameter, 5 mm; depth, 3 mm) was created on the patellar groove of the femur in both legs using a drill and a biopsy punch (Kai Industries, Seki, Japan). The bottom of the subchondral bone was shaved to a plane using the biopsy punch until bleeding was seen from the marrow. Rabbits were classified into two recipient groups: Group B, with administration of bevacizumab (10 rabbits; 100-mg intravenous injection administered on the day of surgery and 2 weeks later); and controls (10 rabbits; defect only). After recovery from surgery, all animals were allowed to walk freely in their cages without any splints.

Histological evaluation of cartilage repair

Rabbits were killed 1 and 3 months postoperatively by an overdose of intravenous anesthetic. The distal part of the femur was excised and fixed with 4% paraformaldehyde for 7 days. Each specimen was decalcified in a solution of 10% ethylenediaminetetraacetic acid (EDTA) in distilled water (pH 7.4) for 2-3 weeks, then embedded in paraffin wax and sectioned perpendicularly (4.5-m sections) through the center of the defect. Each section was stained with safranin O for glycosaminoglycans.

Immunohistochemistry was performed as described previously [23,33]. Briefly, sections were deparaffinized according to standard procedures. Sections were treated with 0.005% proteinase (type XXIV; Sigma-Aldrich Co., St. Louis, MO, USA) for 30 min at 37°C for antigen retrieval. For chondromodulin-I (ChM-I), primary goat polyclonal antibody (Santa Cruz Biotechnology, Santa Cruz, CA, USA) diluted 1:200 in phosphate-buffered saline (PBS) and 1% bovine serum albumin (BSA) was placed on the section overnight at 4°C. For VEGF, a primary mouse monoclonal antibody (Upstate, Lake Placid, NY, USA) diluted 1:50 in PBS and 1% BSA was placed on the section overnight at 4°C. Slides were washed with PBS after incubation for 1 h at room temperature with biotin-conjugated goat antimouse secondary antibody for VEGF and with biotin-conjugated donkey antigoat secondary antibody for ChM-I. Next, slides were treated with horseradish peroxidase-labeled streptavidin for 1 h and then soaked in 0.05% solution of diaminobenzidine in Tris HCl buffer (pH 7.6) containing 0.005% hydrogen peroxide. Finally, slides were counterstained with Mayer's hematoxylin. Safranin O-stained sections were scored by two individuals under blinded conditions, according to a modified O'Driscoll [34] International Cartilage Repair Society (ICRS) grading scale [26] (Table 1).

Statistical analysis

Results are presented as the means ± standard deviation (SD). Histological score was analyzed by the Mann-Whitney U test. Values of $P < 0.05$ were considered statistically significant for any differences.

Results

Histological evaluation of repair tissue

Operations were uneventful, and all rabbits immediately resumed normal cage activity. In Group B, major infection was identified in one knee at 1 month after surgery and in three knees at 3 months. These infected knees were omitted from the study. As a result, nine knees at 1 month and seven knees at 3 months were assessed

Table 1 Histological grading system[a]

Tissue morphology (Ti)	Intactness of calcified cartilage layer, formation of tidemark (Tide)	Lateral integration of implanted material (Latl)
4 = Mostly hyaline cartilage	1 = <25% of the calcified cartilage layer intact	1 = Not bonded
3 = Mostly fibrocartilage	2 = 25-49% of the calcified cartilage layer intact	2 = Bonded at one end/partially both ends
2 = Mostly noncartilage	3 = 50-75% of the calcified cartilage layer intact	3 = Bonded at both sides
1 = Exclusively noncartilage	4 = 76-90% of the calcified cartilage layer intact	**Basal integration of implanted material (Basl)**
Matrix staining (Matx)	5 = Complete intactness of the calcified cartilage layer	1 = <50%
1 = None	**Subchondral bone formation (Bform)**	2 = 50-70%
2 = Slight	1 = No formation	3 = 70-90%
3 = Moderate	2 = Slight	4 = 91-100%
4 = Strong	3 = Strong	**Inflammation (InfH)**
Structural integrity (Stru)	**Histologic appraisal of surface architecture (SurfH)**	1 = Strong inflammation
1 = Severe disintegration	1 = Severe fibrillation	3 = Slight inflammation
2 = Cysts or disruption	2 = Moderate fibrillation	5 = No inflammation
3 = No organization of chondrocytes	3 = Slight fibrillation or irregularity	**Histologic grading system (Hgtot)**
4 = Beginning of columnar organization of chondrocytes	4 = Normal	Some of the histologic variables:
5 = Normal, similar to healthy mature cartilage	**Histologic appraisal defect filling (FilH)**	Tissue morphology (Ti)
Chondrocytes clustering in implant (Clus)	1 = <25%	Matrix staining (Matx)
1 = 25-100% of cells clustered	2 = 26-50%	Structural integrity (Stru)
2 = <25% of the cells clustered	3 = 51-75%	Cluster formation (Clus)
3 = No clusters	4 = 76-90%	Tidemark opening (Tide)
	5 = 91-110%	Bone formation (Bform)
		Histologic surface architecture (SurfH)
		Histologic degree of defect filling (FilH)
		Lateral integration of defect-filling tissue (Basl) and histologic signs of inflammation (InfH)

[a]Presentation of variables and the grading system based on a modified International Cartilage Repair Society (ICRS) grading scale [26] developed by O'Driscoll, Keeley and Salter [34].

from Group B, compared to 10 knees in controls at both 1 and 3 months.

At 1 month after surgery, defects in both Group B and the controls were filled with reparative cells. In Group B, the repair site appeared to be filled with cartilaginous tissue, which was stained with safranin O (Figures 1a and 1b). Lateral integration was well bonded at both sides of the surrounding cartilage. The surface of the repair site showed several smooth fibrous cell layers, and rounded chondrocytes formed inside the repair tissue in a convex pattern. The lower portion of the repair tissue contained hypertrophic chondrocytes that were remodeling the subchondral bone. Thus, the defects showed sequential construction of abundant inhomogeneous extracellular matrix from the surface by fibrous cells (or fibrocartilage cells), rounded chondrocytes and hypertrophic chondrocytes. Similarly, in the controls, defects consisted of inhomogeneous extracellular matrix from fibrous cells (or fibrocartilage cells), rounded chondrocytes and hypertrophic chondrocytes; however, no tendency toward uniform constitution was apparent. The defect was not filled with repaired tissue (Figures 1c and 1d). At 3 months in Group B, the repair site maintained a cartilage phenotype and was well integrated with the surrounding cartilage (Figure 2). Repaired tissue showed a columnar organization. The surface of the repair site retained a smooth and convex formation similar to the surrounding cartilage. In the controls at 3 months, the repair site had been replaced with fibrous tissue and bone (Figure 3), and in the surrounding adjacent cartilage there was evidence of osteoarthritic changes with loss of cartilage.

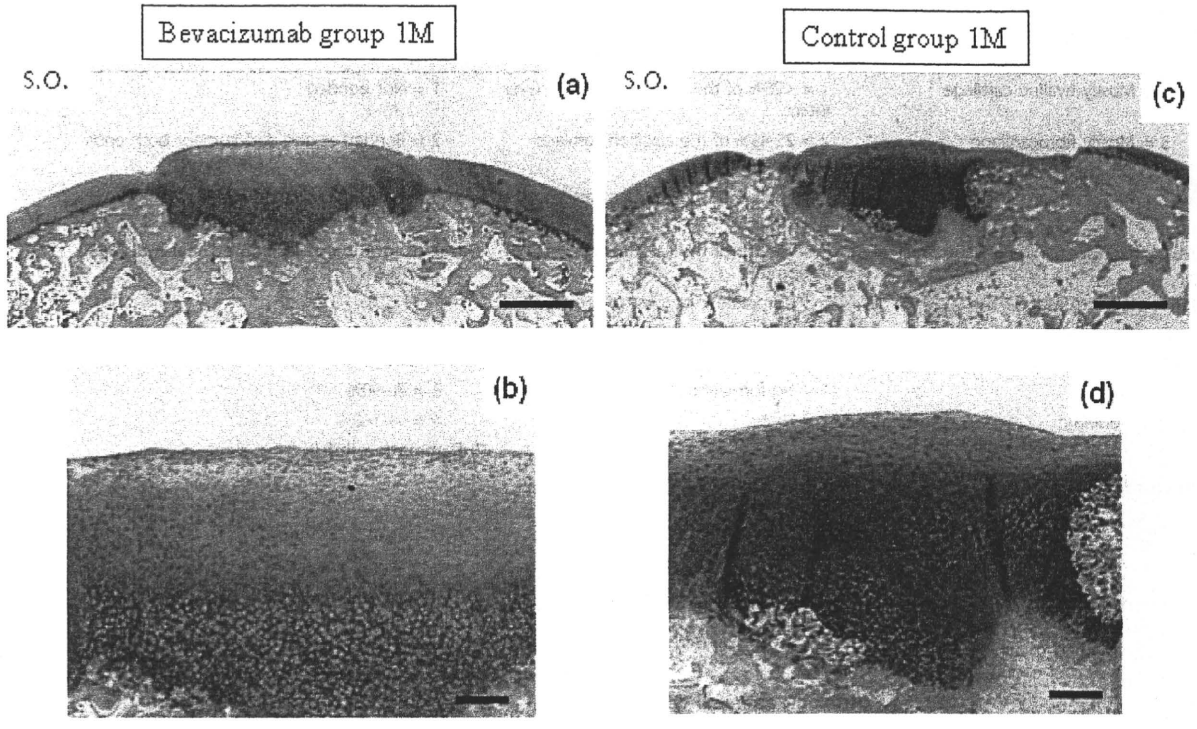

Figure 1 Photomicrographs showing safranin O staining at 1 month after surgery. (a, b) The defect treated with bevacizumab. **(c, d)** The defect untreated as the control. Scale bars, 1 mm in (a) and (c) and 250 μm in (b) and (d).

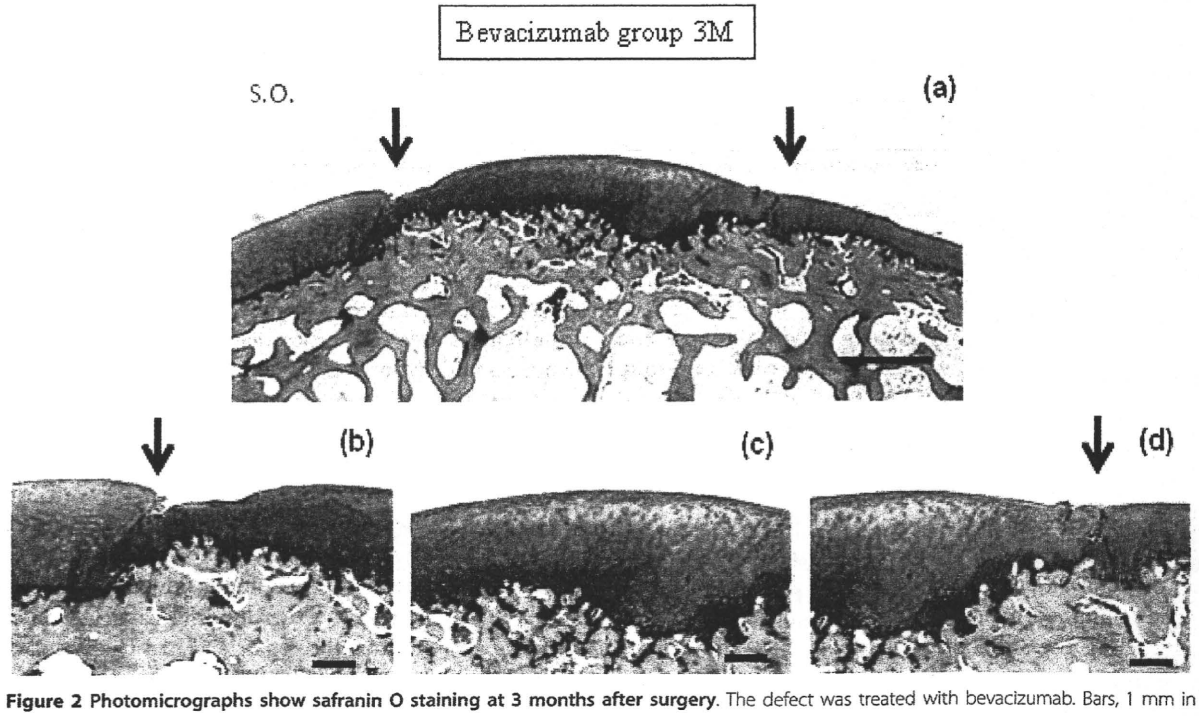

Figure 2 Photomicrographs show safranin O staining at 3 months after surgery. The defect was treated with bevacizumab. Bars, 1 mm in **(a)** and 250 μm in **(b, c** and **d)**.

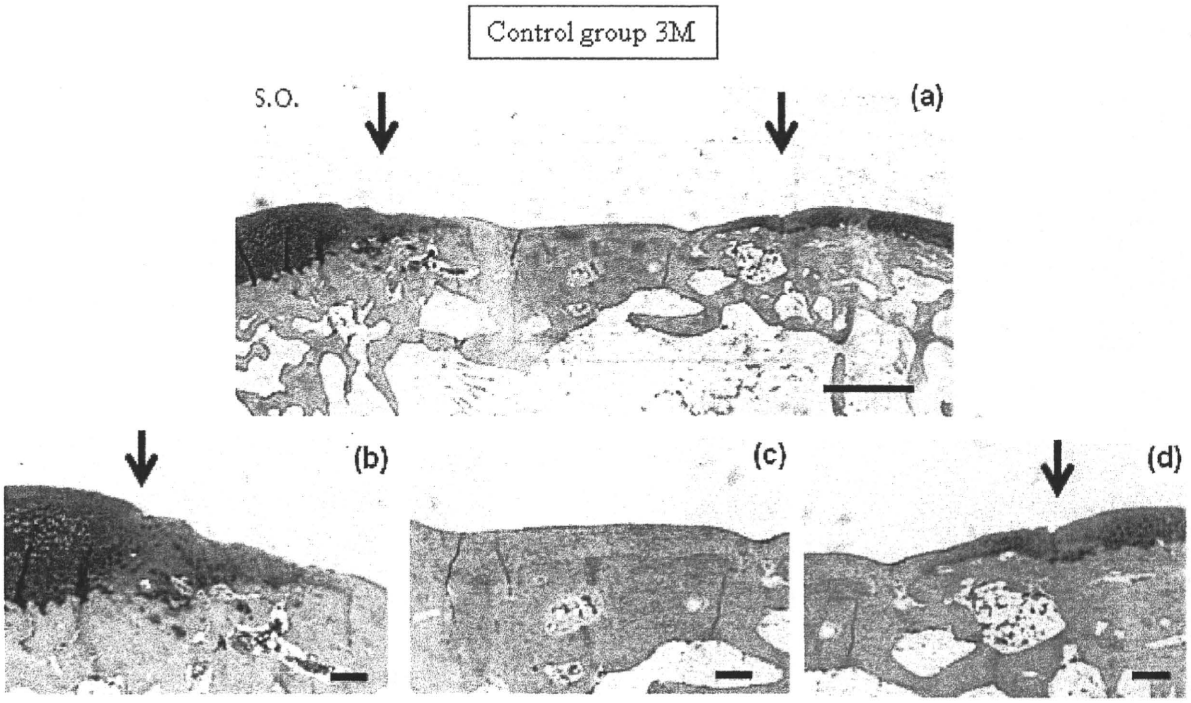

Figure 3 Photomicrographs show safranin O staining at 3 months after surgery. The untreated defect in the control. Bars, 1 mm in **(a)** and 250 μm in **(b, c** and **d)**.

Evaluation of ChM-I and VEGF expression

At 1 month, Group B showed intense positive results for ChM-I at the bottom of the repair tissue in the remodeling hypertrophic chondrocyte layer, representing the border between cartilage and bone (Figure 4a). ChM-I had accumulated in the interterritorial space of the repaired matrix (Figure 4a). In the controls, no ChM-I was observed in the repair tissue (Figure 4b). Conversely, the remodeling hypertrophic chondrocyte layer was intensely positive for VEGF in both Group B and in the controls (Figures 4c and 4d).

Histological scoring of repair tissue

We evaluated the repair site using a modified version of the grading system developed by O'Driscoll, Keeley and Salter [34]. In this system, 11 histologic categories were evaluated and scored: tissue morphology (Ti), matrix staining (Matx), structural integrity (Stru), cluster formation (Clus), tidemark opening (Tide), bone formation (Bform), histologic appraisal of surface architecture (SurfH), histologic appraisal of the degree of defect filling (FilH), lateral integration of defect-filling tissue (Latl), basal integration of defect-filling tissue (Basl) and histologic signs of inflammation (InfH). The total score ranged from 11 (no repair) to 45 (normal articular cartilage) (Table 1).

At 1 month, inside the repair tissue in Group B, Ti was mostly hyaline cartilage in seven of nine cases, with high cellularity of rounded chondrocytes and mostly fibrocartilage in two of nine cases. Conversely, in the controls, 4 of 10 cases showed mostly hyaline cartilage, 4 of 10 cases were mostly fibrocartilage and 2 of 10 cases were mostly noncartilage. For Matx in Group B, six of nine cases were strong, two of nine cases were moderate and one case showed slight staining. In the controls, 5 of 10 cases were strong, 3 of 10 cases were moderate and 2 of 10 cases showed slight staining. In Group B, Stru of the defect filling revealed the beginning of columnar organization of chondrocytes in six of nine cases and no organization of chondrocytes in three of nine cases. In the controls, 3 of 10 cases showed the beginning of columnar organization, 4 of 10 cases showed no organization and 3 of 10 cases showed cysts or disruptions. In both groups, Clus was not observed except in one instance. In one instance, there was a small amount of Clus in both groups. Also, in both groups, Tide was opened in all instances. In Group B, subchondral Bform was not recognized in four of nine cases, slightly recognized in four of nine cases and strongly recognized in one of nine cases. In the control group, subchondral Bform was not recognized in 8 of 10 cases and was slightly recognized in 2 of 10 cases.

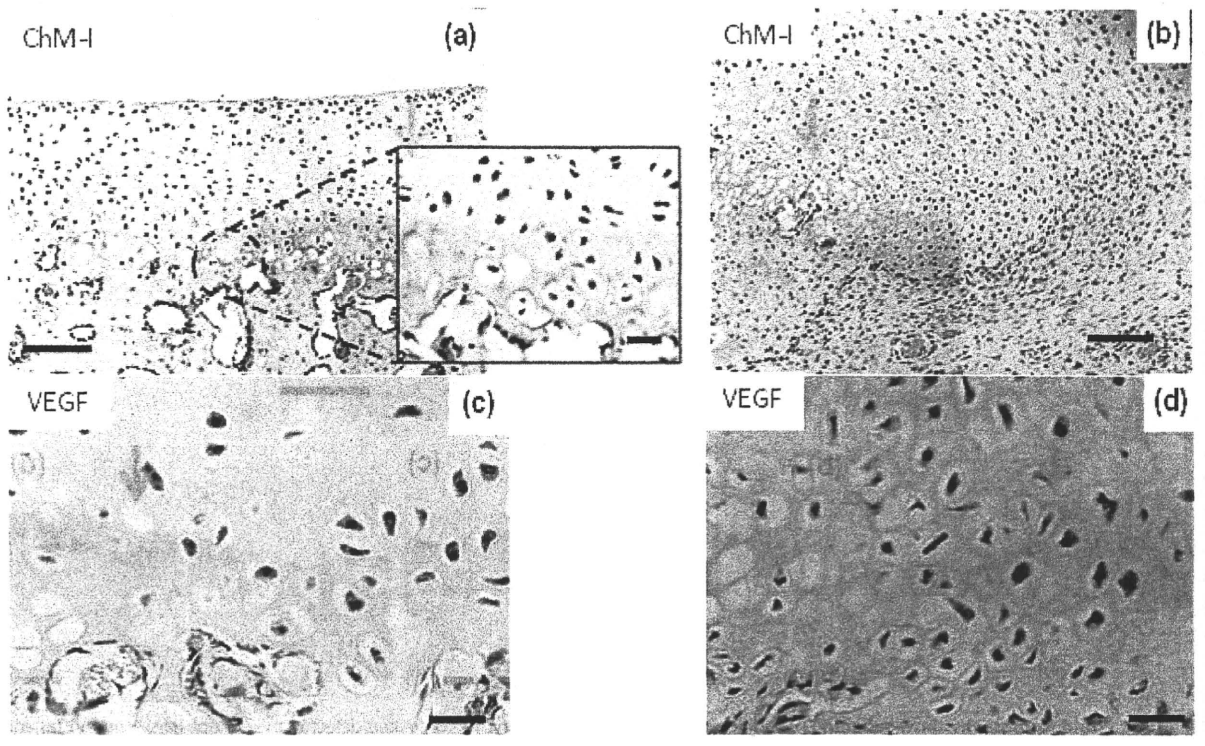

Figure 4 Chondromodulin (ChM)-I and vascular endothelial growth factor (VEGF) localized in cartilage at 1 month after surgery. (a, c) The defect treated with bevacizumab. **(b, d)** The defect in the control. (a) In the bevacizumab group, ChM-I immunostaining is detected in the interterritorial matrix of the remodeling site. (b) In the control group, ChM-I immunostaining is not detected in the remodeling site. (c, d) In both groups, VEGF immunostaining is detected in the remodeling site of the reparative cells. Bars, 100 μm in (a) and (b) and 25 μm in (c) and (d).

SurfH in Group B was normal in five of nine cases and showed slight fibrillation or irregularity in four of nine cases; in the control group, 1 of 10 cases was normal, 6 of 10 cases showed slight fibrillation or irregularity, 2 of 10 cases showed moderate fibrillation or irregularity and 1 of 10 cases showed severe fibrillation or disruption. FilH in Group B was complete in six of nine cases and nearly complete in three of nine cases. In controls, FilH was complete in 2 of 10 cases, nearly complete in 4 of 10 cases, moderate in 2 of 10 cases and nearly empty in 2 of 10 cases. Latl in Group B was bonded on both sides in seven of nine cases and bonded at one end or partially at both ends in two of nine cases. In controls, Latl was bonded on both sides in 1 of 10 cases, bonded at one end or partially at both ends in 6 of 10 cases and not bonded in 3 of 10 cases. Basl was good in all cases for both groups. In Group B, no inflammation was observed in all cases for InfH. The control group showed no inflammation in 5 of 10 cases, slight inflammation in 4 of 10 cases and strong inflammation in 1 of 10 cases. As a result, at 1 month, the total score was significantly higher for Group B than for the controls. In terms of individual scores, SurfH, FilH and Latl for Group B were significantly higher than in controls.

In Group B, Ti at 3 months showed mostly hyaline cartilage in six of seven cases. In one of seven cases, tissue was mostly fibrocartilage. Conversely, in the controls, 3 of 10 cases were mostly hyaline cartilage, with mostly fibrocartilage in 1 of 10 cases and exclusively noncartilage in 6 of 10 cases. For Matx, six of seven cases in Group B showed strong staining and one of seven cases showed moderate staining; in the controls, 3 of 10 cases were strong, one instance was moderate and 6 of 10 cases were nonstaining. In Group B, Stru of the defect filling revealed tissue similar to healthy mature cartilage in three of seven cases, beginning columnar organization of chondrocytes in three of seven cases and no organization of the chondrocytes in one of seven cases. In the controls, only one instance was similar to healthy mature cartilage, 2 of 10 cases were beginning columnar organization, 1 of 10 cases had no organization and 6 of 10 cases showed severe disintegration. In Group B, Clus was not observed. In controls, 2 of 10 cases showed no clusters, 2 of 10 cases showed some clusters and 6 of 10 cases showed abundant cluster cells or nonchondrocytes. Tide in Group B was complete in three of seven cases, nearly complete in two of seven cases, half degree in one of seven cases and nearly

absent in one of seven cases; in the controls, 1 of 10 cases was complete, 2 of 10 cases were nearly complete, 1 of 10 cases was half degree and 6 of 10 cases were not recognized as containing a calcified cartilage layer. Bform was recognized in both groups, except for one instance in each. In one instance, there was a slightly Bform in both groups. SurfH in Group B was normal in five of seven cases and showed slight fibrillation or irregularity in two of seven cases; in the controls, 1 of 10 cases was normal, 1 of 10 cases showed slight fibrillation or irregularity, 2 of 10 cases showed moderate fibrillation or irregularity and 6 of 10 cases showed severe fibrillation or disruption. FilH in Group B was complete in all instances. In the controls, FilH was complete in 4 of 10 cases, moderate in 1 of 10 cases, nearly empty in 1 of 10 cases and almost empty in 4 of 10 cases. Latl in Group B were bonded at both sides in six of seven cases and bonded at one end in one of seven cases. In the controls, Latl was bonded both sides in 1 of 10 cases, bonded at one end or partially both ends in 2 of 10 cases and not bonded in 6 of 10 cases. Basl was good in all cases in both groups. For InfH, no inflammation was observed in any cases in either group. At 3 months, the total score for Group B was significantly higher than that for the controls. In terms of individual scores, Ti, Matx, Stru, Clus, SurfH, FilH and Latl were significantly higher for Group B than for the control group (Table 2).

Discussion

VEGF is overexpressed in numerous solid angiogenic tumors and hematological malignancies. Interrupting the VEGF pathway has thus become a major focus of oncology research [35]. The first approved antiangiogenic therapy was bevacizumab, a humanized monoclonal anti-VEGF antibody. Following the success of a pivotal trial, the FDA approved bevacizumab for use in combination with intravenous 5-fluorouracil-based chemotherapy as a treatment for patients with first-line or previously untreated metastatic cancer of the colon or rectum [36]. Bevacizumab is anticipated to be useful not only for cancer treatment but also as a major advance in antiangiogenic therapy.

Table 2 Histological scores for cartilage repair at 1 month and 3 months after surgery[a]

	1 month		3 months	
	Group B	Control	Group B	Control
Ti	3.77 ± 0.4	3.20 ± 0.7	3.85 ± 0.3*	2.10 ± 1.4
Matx	3.55 ± 0.7	3.30 ± 0.8	3.71 ± 0.7*	2.10 ± 1.4
Stru	3.66 ± 0.5	3.00 ± 0.8	4.28 ± 0.7*	2.41 ± 1.6
Clus	2.88 ± 0.3	2.90 ± 0.3	3.00 ± 0.0*	1.60 ± 0.8
Tide	1.00 ± 0.0	1.00 ± 0.0	3.85 ± 1.4	2.20 ± 1.6
Bform	1.66 ± 0.7	1.20 ± 0.4	2.85 ± 0.3	2.90 ± 0.3
SurfH	3.55 ± 0.5*	2.70 ± 0.8	3.71 ± 0.4*	1.70 ± 1.0
FilH	4.66 ± 0.5*	3.70 ± 1.0	5.00 ± 0.0*	2.90 ± 1.9
Latl	2.77 ± 0.4*	1.80 ± 0.6	2.85 ± 0.3*	1.60 ± 0.8
Basl	4.00 ± 0.0	4.00 ± 0.0	4.00 ± 0.0	4.00 ± 0.0
InfH	5.00 ± 0.0	3.80 ± 1.3	5.00 ± 0.0	5.00 ± 0.0
Hgtot	36.55 ± 2.1*	30.50 ± 4.1	40.14 ± 2.5*	27.7 ± 10.0

[a]Values are means ± SD. The total score range is from 11 (no repair) to 45 (normal articular cartilage).

*Denotes significance at $P < 0.05$.

Generally, osteochondral defects have access to reparative cells of the bone marrow [37]. This connection allows infiltration of the bone by mesenchymal stem cells (MSCs) from the bone marrow, which can then proliferate and differentiate. MSC-derived chondrocytes subsequently appear during endochondral ossification and are invaded by the vasculature and marrow, and eventually the defects are replaced by subchondral bone [28,38]. In summary, MSC-derived chondrocytes are spontaneously recruited as reparative cells in osteochondral defects and are replaced by bone with high levels of vascular invasion. However, articular cartilage is a naturally avascular tissue, except during skeletal development, when endochondral bone formation occurs. We speculate that MSCs may use different courses of differentiation to become bone or cartilage, based on environmental differences in vascularization and avascularization. We recently reported that MSCs that acquire antiangiogenic properties achieve good cartilage restoration [23]. Furthermore, previous research has shown that VEGF expression by chondrocytes in osteoarthritic joints may be related to articular cartilage destruction [39-46]. High-dose VEGF may induce the onset and progression of arthritis [47,48]. Also, expression of high levels of VEGF during the terminal stages of chondrogenesis leads to endochondral ossification through angiogenesis [49,50]. We therefore studied the restoration of articular cartilage by blocking VEGF signaling with bevacizumab in a model of osteochondral defects in Japanese white rabbits.

At 1 month after surgery in both Group B and the controls, defects were recruited with reparative cells from the marrow and synovial tissue, and this was composed of differentiated chondrocytes, hyperchondrocytes and fibrous cells. These heterogeneous cells stained positive for safranin O and showed various levels of structured organization. From the surface, these structures consisted of a fibrous or fibrocartilage layer, a hyaline cartilage layer and a hypertrophic chondrocyte layer in both groups. As a result, no significant differences were apparent between the two groups at 1 month postoperatively in Ti, Matx or Stru. However, at 1 month after surgery, the defects were repaired by hyaline cartilage (seven of nine cases) in Group B, a result of blocking VEGF, whereas in the controls, the defects were repaired with that of various tissues, including hyaline

cartilage (4 of 10 cases), fibrocartilage (4 of 10 cases) and noncartilage (2 of 10 cases). There was no delay in subchondral bone formation in Group B when blocking VEGF. For autologous reparative cells, basal integration was good and most inflammatory signs were absent from both groups. On the other hand, FilH, Latl and SurfH were significantly higher for Group B than for the controls. Actually, at 1 month after surgery, six of nine cases in Group B showed convex surfaces of these repaired tissues in surrounding articular cartilage, compared to only 2 of 10 cases in the controls. These results indicate that blocking VEGF preserves the accumulation of reparative cells in the defect. This is supported by studies showing that VEGF treatment prevents condensation of chondrogenic mesenchyme during early limb bud development through abnormal vascularization [51]. As a sufficient number of reparative cells made contact with the surrounding cartilage layer, lateral integration was considered to be good. Also, repaired tissue taking a convex form consisted of a smoother surface than repaired tissue with a concave form.

Defects had been repaired by the formation of various tissues in the controls at 3 months after surgery, which included hyaline cartilage (3 of 10 cases), fibrocartilage (1 of 10 cases) and exclusively noncartilage (6 of 10 cases). On the other hand, when blocking VEGF, defects were repaired mostly with hyaline cartilage (six of seven cases), with only one case being mostly fibrocartilage. To emphasize this, no cases showed replacement by fibrous tissue or bone. Similarly, 1 month after surgery, the controls showed repair without consistent tissue morphology, while Group B showed repair with consistency of tissue morphology. At 3 months postoperatively, Ti, Matx, Stru and Clus were significantly higher for Group B than for the controls. In both Group B and the controls, Tide was generally closed and bone formation was gradually observed. Continuous basal integration was also good and most signs of inflammation were not apparent in either group. Tissue that was repaired in the form of fibrous tissue and bone tended to show moderate or severe fibrillation of surface architecture and low defect filling. Therefore, SurfH and FilH were significantly higher for Group B than for the controls. As mentioned before, a sufficient number of reparative cells were in contact with the surrounding cartilage layer, and lateral integration was considered to be good. As a result, at 3 months, the total score was significantly higher for Group B than for the controls.

Interestingly, ChM-I was expressed in the early stage of tissue repair after bevacizumab administration. ChM-I reportedly stimulates chondrocyte proliferation and proteoglycan synthesis in vitro and inhibits proliferation of vascular endothelial cells in vitro and in vivo [52,53]. Kitahara *et al.* [53] suggested that in their mouse model, ChM-I acts to inhibit vascular invasion in the immature state of articular cartilage, and levels of ChM-I gradually decrease with age thereafter. Hiraki *et al.* [52] reported that ChM-I is expressed in the avascular zone of cartilage in developing bone, but is not present in calcifying cartilage. Such findings suggest a regulatory role of ChM-I in vascular invasion during endochondral bone formation.

In this study, ChM-I was expressed at the bottom of the repair site invaded near the vasculature. ChM-I accumulated in the interterritorial space of the repaired matrix and was surrounding the cells that expressed VEGF. ChM-I is thought to form a barrier to inhibit vascular invasion from subchondral bone, indicating that it facilitates the acquisition of articular cartilage through the process of MSC differentiation in endochondral ossification. However, the shift from angiogenesis to antiangiogenesis is not determined entirely by ChM-I and VEGF. Inducers of endogenous angiogenic molecules also exist in the process of endochondral ossification, and these include VEGF [53], fibroblast growth factor 2 [54], transforming growth factor [55] and tissue matrix metalloprotease 9 [56].

In other studies, VEGF has been reported to be necessary for chondrocyte survival during cartilage development. In VEGF-deficient mouse models, massive cell death is observed in the joint and epiphyseal regions of cartilage during cartilage development [57,58]. In this study, we blocked VEGF temporarily to initiate reparative cells. To avoid complete inhibition of the bioactivity of VEGF in reparative cells, we blocked VEGF on the day of surgery and 2 weeks later. As a result, 1 month after surgery, reparative cells actually expressed VEGF in Group B (Figure 4c). Moreover, expression of ChM-I as an antiangiogenic factor was observed in the layer of reparative cells involved in blood vessel invasion from subchondral bone (Figure 4a). It is important to consider the efficacy of various VEGF treatments in the balance of angiogenesis-antiangiogenesis during chondrogenic differentiation of MSC-derived reparative cells. In other words, repair of articular cartilage may be achievable by adjusting optimal VEGF signaling. In a recent study, Kubo *et al.* [39] reported good cartilage restoration using muscle-derived stem cells that transfected with the genes of Flt-1 (a VEGF antagonist) and bone morphogenetic protein (BMP) 4 in a mouse osteochondral defect model. However, the techniques applied in that study were complicated, as they required isolation of stem cells from muscular tissue, gene transduction and cell culture in vitro, as well as cell transplantation. Conversely, the present technique involves the simple means of achieving cartilage restoration by intravenous administration of bevacizumab, a treatment already cleared for clinical application. Hence,

this method would be applicable in many medical facilities. Thus, vascularization of the tissue environment after injury or degeneration would be improved to a more advantageous situation of cartilage repair if VEGF were blocked. Accordingly, without depending on cells or tissue transplantation, this approach would augment the curative effects of existing approaches such as microfracture or drilling.

The half-life of bevacizumab in the circulation of humans is reportedly 17-21 days. The approved dose of bevacizumab in humans is 5 mg/kg, and the clinical administration interval is more than 2 weeks [30]. Bevacizumab is cross-reactive with rabbit VEGF, but has eightfold lower affinity for rabbit VEGF than for human VEGF [59]. Therefore, in this study, we investigated bevacizumab at the dose of 40 mg/kg administered on the day of surgery and 2 weeks later. As a future consideration, we plan to investigate the dosage and duration of bevacizumab administration. We will also address the side effects of infection by applying minimally invasive surgery with an arthroscope and using antibiotics.

Conclusions

Temporary intravenous administration of the humanized monoclonal anti-VEGF antibody bevacizumab in an osteochondral defect model results in positive restorative effects. We suggest that this approach would be useful to achieve repair of articular cartilage without the need for cells or tissue transplantation.

Abbreviations

BASL: basal integration of defect-filling tissue; BFORM: bone formation; BMP: bone morphogenetic protein; BSA: bovine serum albumin; CHM-I: chondromodulin-I; CLUS: cluster formation; EDTA: ethylenediaminetetraacetic acid; FILH: histologic appraisal of the degree of defect filling; ICRS: International Cartilage Repair Society; INFH: histologic signs of inflammation; LATL: lateral integration of defect-filling tissue; MATX: matrix staining; PBS: phosphate-buffered saline; SD: standard deviation; STRU: structural integrity; SURFH: histologic appraisal of surface architecture; TI: tissue morphology; TIDE: tidemark opening; VEGF: vascular endothelial growth factor.

Acknowledgements

This research was partly supported by Grants-In-Aid for Scientific Research from the Ministry of Education, Culture, Sports, Science and Technology of Japan, and Mitsui Sumitomo Insurance Welfare Foundation.

Authors' contributions

TN and MS performed most of the experiments and MK performed the immunohistochemistry. TK, GE and NO helped with in vivo experiments. TN performed statistical analyses. MS and JM designed and coordinated the study and helped draft the manuscript. All authors approved the final manuscript.

Competing interests

The authors declare that they applied for a patent relating to the content of the manuscript in Japan, but did not receive any reimbursements, fees, funding or salary from an organization. The competitive companies developing or selling anti-VEGF drugs (e.g., Novartis, Wyeth, Bayer Schering) may keep them in check.

Received: 17 May 2010 Revised: 31 July 2010
Accepted: 24 September 2010 Published: 24 September 2010

References

1. Paget J: **Healing of cartilage.** *Clin Orthop Relat Res* 1969, **64**:7-8.
2. Pridie KH: **A method of resurfacing osteoarthritic knee joints.** *J Bone Joint Surg Br* 1959, **41**:618-619.
3. Muller B, Kohn D: **Indication for and performance of articular cartilage drilling using the Pridie method.** *Orthopade* 1999, **28**:4-10.
4. Insall JN: **Intra-articular surgery for degenerative arthritis of the knee. A report of the work of the late K. H. Pridie.** *J Bone Joint Surg Br* 1967, **49**:211-228.
5. Insall J: **The Pridie debridement operation for osteoarthritis of the knee.** *Clin Orthop* 1974, **101**:61-67.
6. Steadman J, Rodkey W, Briggs K, Rodrigo J: **The microfracture technique in the management of complete cartilage defects in the knee joint.** *Orthopade* 1999, **28**:26-32.
7. Steadman J, Rodkey W, Rodrigo J: **Microfracture: surgical technique and rehabilitation to treat chondral defects.** *Clin Orthop Relat Res* 2001., **391 Suppl**: S362-S369.
8. Steadman J, Rodkey W, Briggs K: **Microfracture to treat full-thickness chondral defects: surgical technique, rehabilitation, and outcomes.** *J Knee Surg* 2002, **15**:170-176.
9. Mithoefer K, Williams RJ, Warren RF, Potter HG, Spock CR, Jones EC, Wickiewicz TL, Marx RG: **Chondral resurfacing of articular cartilage defects in the knee with the microfracture technique: surgical technique.** *J Bone Joint Surg Am* 2006, **88**:294-304.
10. Hangody L, Kish G, Karpati Z, Udvarhelyi I, Szerb I, Bely M: **Autogenous osteochondral graft technique for replacing knee cartilage defects in dogs.** *Orthopedics* 1997, **5**:175-181.
11. Hangody L, Feczko P, Bartha L, Bodo G, Kish G: **Mosaicplasty for the treatment of articular defects of the knee and ankle.** *Clin Orthop Relat Res* 2001., **391 Suppl**: S328-S336.
12. Szerb I, Hangody L, Duska Z, Kaposi NP: **Mosaicplasty: long-term follow-up.** *Bull Hosp Jt Dis* 2005, **63**:54-62.
13. Brittberg M, Lindahl A, Nilsson A, Ohlsson C, Isaksson O, Peterson L: **Treatment of deep cartilage defects knee with autologus chondrocyte transplantation.** *N Engl J Med* 1994, **331**:889-895.
14. Peterson L, Minas T, Brittberg M, Lindahl A: **Treatment of osteochondritis dissecans of the knee with autologouschondrocyte transplantation: results at two to ten years.** *J Bone Joint Surg Am* 2003, **85-A Suppl 2**:17-24.
15. Zaslav K, Cole B, Brewster R, DeBerardino T, Farr J, Fowler P, Nissen C, STAR Study Principal Investigators: **A prospective study of autologous chondrocyte implantation in patients with failed prior treatment for articular cartilage defects of the knee: results of the Study of the Treatment of Articular Repair (STAR) clinical trial.** *Am J Sports Med* 2009, **37**:42-55.
16. Moseley JB Jr, Anderson AF, Browne JE, Mandelbaum BR, Micheli LJ, Fu F, Erggelet C: **Long-term durability of autologus chondrocyte implantation: a multicenter, observational study in US patients.** *Am J Sports Med* 2010, **38**:238-46.
17. Darling EM, Athanasiou KA: **Articular cartilage bioreactor and bioprocess.** *Tissue Eng* 2003, **9**:9-26.
18. Backwalter JA, Lohmander S: **Operative treatment of osteoarthrosis. Current practice and future development.** *J Bone Joint Surg Am* 1994, **76**:1405-1418.
19. Freed LE, Grande DA, Lingbin Z, Emmanual J, Marquis JC, Langer R: **Joint resurfacing using allograft chondrocytes and synthetic biodegradable polymer scaffolds.** *J Biomed Mater Res* 1994, **28**:891-899.
20. Hunziker EB: **Articular cartilage repair: basic science and clinical progress. A review of the current status and prospects.** *Osteoarthritis Cartilage* 2002, **10**:432-463.
21. Marcacci M, Berruto M, Brocchetta D, Delcogliano A, Ghinelli D, Gobbi A, Kon E, Pederzini L, Rosa D, Sacchetti GL, Stefani G, Zanasi S: **Articular cartilage engineeiring with Hyalograft C: 3-year clinical results.** *Clin Orthop Relat Res* 2005, **435**:96-105.
22. Crawford DC, Heveran CM, Cannon WD Jr, Foo LF, Potter HG: **An autologus cartilage tissue implant NeoCart for treatment of grade III chondral injury to the distal femur: prospective clinical safety trial at 2 years.** *Am J Sports Med* 2009, **37**:1334-1343.

23. Nagai T, Sato M, Furukawa KS, Kutsuna T, Ohta N, Ushida T, Mochida J: **Optimization of allograft implantation using scaffold-free chondrocyte plates.** *Tissue Eng Part A* 2008, **14**:1225-1235.
24. Nagai T, Furukawa KS, Sato M, Ushida T, Mochida J: **Characteristics of a scaffold-free articular chondrocyte plate grown in rotational culture.** *Tissue Eng Part A* 2008, **14**:1183-1193.
25. Mainil-Varlet P, Rieser F, Grogan S, Mueller W, Saager C, Jakob RP: **Articular cartilage repair using a tissue-engineered cartilage-like implant: an animal study.** *Osteoarthritis Cartilage* 2001, **9 Suppl A**:S6-S15.
26. Brehm W, Aklin B, Yamashita T, Rieser F, Trub T, Jakob RP, Mainil-Varlet P: **Repair of superficial osteochondral defects with an autologous scaffold-free cartilage construct in a caprine model: implantation method and short-term results.** *Osteoarthritis Cartilage* 2006, **14**:1214-1226.
27. Park K, Huang J, Azar F, Jin RL, Min BH, Han DK, Hasty K: **Scaffold-free, engineered porcine cartilage construct for cartilage defect repair: in vitro and in vivo study.** *Artif Organs* 2006, **30**:586-596.
28. Caplan AI, Elyaderani M, Mochizuki Y, Wakitani S, Goldberg VM: **Principles of cartilage repair and regeneration.** *Clin Orthop Relat Res* 1997, **342**:254-272.
29. Nagai T, Sato M, Furukawa KS, Kutsuna T, Ohta N, Ushida T, Mochida J: **Repair of total thickness defect of articular cartilage with scaffold-free chondrocyte plate.** *Proceedings of 55th Annual Meeting, Orthopaedic Research Society, 22-25 February* Las Vegas, NV, USA 2009.
30. Herbert H, Louis F, William N, Thomas C, John H, William H, Jordan B, Ari B, Susan G, Eric H, Napoleone F, Gwen F, Beth R, Robert R, Fairooz K: **Bevacizumab plus Irinotecan, Fluorouracil, and Leucovorin for metastatic colorectal cancer.** *N Engl J Med* 2004, **350**:2335-2342.
31. Jain RK: **Normalizing tumor vasculature with anti-angiogenic therapy: a new paradigm for combination therapy.** *Nat Med* 2001, **7**:987-989.
32. Willet CG, Boucher Y, Di Tomaso E, Duda DG, Munn LL, Tong RT, Chung DC, Sahani DV, Kalva SP, Kozin SV, Mino M, Cohen KS, Scadden DT, Hartford AC, Fischman AJ, Clark JW, Ryan DP, Zhu AX, Blaszkowsky LS, Chen HX, Shellito PC, Lauwers GY, Jain RK: **Direct evidence the VEGF-specific antibody bevacizumab has antivascular effects in human rectal cancer.** *Nat Med* 2004, **10**:145-147.
33. Hayami T, Funaki H, Yaoeda K, Mitui K, Yamagiwa H, Tokunaga K, Hatano H, Kondo J, Hiraki Y, Yamamoto T, Duong le T, Endo N: **Expression of the cartilage derived anti-angiogenic factor chondromodulin-I decreases in the early stage of experimental osteoarthritis.** *J Rheumatol* 2003, **30**:2207-2217.
34. O'Driscoll SW, Keeley FW, Salter RB: **Durability of regenerated articular cartilage produced by free autogenous periosteal grafts in major full-thickness defects in joint surfaces under the influence of continuous passive motion: a follow-up report at one year.** *J Bone Joint Surg Am* 1998, **70**:595-606.
35. Eskens FA: **Angiogenesis inhibitors in clinical development.** *Br J Cancer* 2004, **90**:1-7.
36. Branavan S, Lorraine EH, Ewa MP: **Modulation angiogenesis.** *JAMA* 2004, **292**:972-977.
37. Solchaga LA, Yoo JU, Lundberg M, Dennis JE, Huibregtse BA, Goldberg VM, Caplan AI: **Hyaluronan-based polymers in the treatment of osteochondral defects.** *J Orthop Res* 2000, **18**:773-780.
38. Shapiro F, Koide S, Glimcher MJ: **Cell origin and differentiation in the repair of full-thickness defects of articular cartilage.** *J Bone Joint Surg Am* 1993, **75**:532-553.
39. Kubo S, Cooper GM, Matsumoto T, Phillippi JA, Corsi KA, Usas A, Li G, Fu FH, Huard J: **Blocking vascular endothelial growth factor with soluble Flt-1 improves the chondrogenic potential of mouse skeletal muscle-derived stem cells.** *Arthritis Rheum* 2009, **60**:155-165.
40. Hashimoto S, Ochs RL, Komiya S, Lotz M: **Linkage of chondrocyte apoptosis and cartilage degradation in human osteoarthritis.** *Arthritis Rheum* 1998, **41**:1632-1638.
41. Hashimoto S, Creighton-Achermann L, Takahashi K, Amiel D, Coutts RD, Lotz M: **Development and regulation of osteophyte formation during experimental osteoarthritis.** *Osteoarthritis Cartilage* 2002, **10**:180-187.
42. Enomoto H, Inoki I, Komiya K, Shiomi T, Ikeda E, Obata K, Matsumoto H, Toyama Y, Okada Y: **Vascular endothelial growth factor isoforms and their receptors are expressed in human osteoarthritic cartilage.** *Am J Pathol* 2003, **162**:171-181.
43. Tanaka E, Aoyama J, Miyauchi M, Takata T, Hanaoka K, Iwabe T, Tanne K: **Vascular endothelial growth factor plays an important autocrine/paracrine role in the progression of osteoarthritis.** *Histochem Cell Biol* 2005, **123**:275-281.
44. Pufe T, Petersen W, Tillmann B, Mentlein R: **The splice variants VEGF121 and VEGF189 of the angiogenic peptide vascular endothelial growth factor are expressed in osteoarthritic cartilage.** *Arthritis Rheum* 2001, **44**:1082-1088.
45. Pufe T, Harde V, Petersen W, Goldring MB, Tillmann B, Mentlein R: **Vascular endothelial growth factor (VEGF) induces matrix metalloproteinase expression in immortalized chondrocytes.** *J Pathol* 2004, **202**:367-374.
46. Pufe T, Lemke A, Kurz B, Petersen W, Tillmann B, Grodzinsky AJ, Mentlein R: **Mechanical overload induces VEGF in cartilage discs via hypoxia-inducible factor.** *Am J Pathol* 2004, **164**:185-192.
47. Murakami M, Iwai S, Hiratsuka S, Yamauchi M, Nakamura K, Iwakura Y, Shibuya M: **Signaling of vascular endothelial growth factor receptor-1 tyrosine kinase promotes rheumatoid arthritis through activation of monocytes/macrophages.** *Blood* 2006, **108**:1849-1856.
48. Afuwape AO, Kiriakidis S, Paleolog EM: **The role of the angiogenic molecule VEGF in the pathogenesis of rheumatoid arthritis.** *Histol Histopathol* 2002, **17**:961-972.
49. Gerber HP, Vu TH, Ryan AM, Kowalski J, Werb Z, Ferrara N: **VEGF couples hypertrophic cartilage remodeling, ossification and angiogenesis during endochondral bone formation.** *Nat Med* 1999, **5**:623-628.
50. Carlevaro MF, Cermelli S, Cancedda R, Descalzi Cancedda F: **Vascular endothelial growth factor (VEGF) in cartilage neovascularization and chondrocyte differentiation: auto-paracrine role during endochondral bone formation.** *J Cell Sci* 2000, **113**:59-69.
51. Yin M, Pacifici M: **Vascular regression is required for mesenchymal condensation and chondrogenesis in the developing limb.** *Dev Dyn* 2001, **222**:522-533.
52. Hiraki Y, Inoue H, Iyama K, Kamizono A, Ochiai M, Shukunami C, Iijima S, Suzuki F, Kondo J: **Identification of chondromodulin I as a novel endothelial cell inhibitor: purification and its localization in the avascular zone of epiphyseal cartilage.** *J Biol Chem* 1997, **272**:32419-32426.
53. Kitahara H, Hayami T, Tokunaga K, Endo N, Funaki H, Yoshida Y, Yaoita E, Yamamoto T: **Chondromodulin-I expression in rat articular cartilage.** *Arch Histol Cytol* 2003, **66**:221-228.
54. Gonzalez AM, Buscaglia M, Ong M, Baird A: **Distribution of basic fibroblast growth factor in the 18-day rat fetus: localization in the basement membranes of diverse tissues.** *J Cell Biol* 1990, **110**:753-765.
55. Gelb DE, Rosier RN, Puzas JE: **The production of transforming growth factor-beta by chick growth plate chondrocytes in short term monolayer culture.** *Endocrinology* 1990, **127**:1941-1947.
56. Thiennu HV, Shipley JM, Bergers G, Burger JE, Helms JA, Hanahan D, Shapiro SD, Senior RM, Werb Z: **MMP-9/Gelatinase B is a key regulator of growth plate angiogenesis and apoptosis.** *Cell* 1998, **93**:411-422.
57. Zelzer E, Mamluk R, Ferrara N, Johnson RS, Schipani E, Olsen BR: **VEGFA is necessary for chondrocyte survival during bone development.** *Development* 2004, **131**:2161-2171.
58. Haigh JJ, Gerber HP, Ferrara N, Wagner EF: **Conditional inactivation of VEGF-A in areas of collagen2a1 expression results in embryonic lethality in the heterozygous state.** *Development* 2000, **127**:1445-1453.
59. Van der Flier M, Coenjaerts FE, Mwinzi PN, Rijkers E, Ruyken M, Scharringa J, Kimpen JLL, Hoepelman AIM, Geelen SPM: **Antibody neutralization of vascular endothelial growth factor (VEGF) fails to attenuate vascular permeability and brain edema in experimental pneumococcal meningitis.** *J Neuroimmunol* 2005, **160**:170-177.

doi:10.1186/ar3142
Cite this article as: Nagai *et al.*: **Intravenous administration of anti-vascular endothelial growth factor humanized monoclonal antibody bevacizumab improves articular cartilage repair.** *Arthritis Research & Therapy* 2010 **12**:R178.

Lee et al. BMC Biotechnology 2011, 11:19
http://www.biomedcentral.com/1472-6750/11/19

BMC Biotechnology

RESEARCH ARTICLE Open Access

Measurement of diffusion in articular cartilage using fluorescence correlation spectroscopy

Jeong Ik Lee[1,2], Masato Sato[1*], Kiminori Ushida[3], Joji Mochida[1]

Abstract

Background: Fluorescence correlation spectroscopy (FCS) provides information about translational diffusion of fluorescent molecules in tiny detection volumes at the single-molecule level. In normal states, cartilage tissue lacks vascularity, so chondrocyte metabolism depends on diffusion for molecular exchanges. The abundant extracellular matrix (ECM) of cartilage is maintained by a limited number of chondrocytes. ECM plays an important role in the regulation of chondrocyte functions. In this study, FCS was used to measure diffusion behaviors of albumin, the major protein of the intra-articular space, using normal and degenerated cartilage. Preliminary investigation of fluorescence dyes including Alexa 488, Rhodamine 6G and Rhodamine 123 was conducted to evaluate their properties in cartilage.

Results: The results indicate that the diffusion behaviors of fluorescently labeled albumin can be observed using FCS in both normal and chemically degenerated cartilage.

Conclusions: This work demonstrates the capability of FCS for direct measurement of diffusion in cartilaginous ECM. When the diffusion characteristics of fluorescent probes in ECM are clarified using FCS evaluation, FCS will be applicable as a method for early diagnosis of osteoarthritis, which is accompanied by increased abnormalities of ECM and also as tool for evaluating bio-engineered artificial cartilage for autologous chondrocyte implantation.

Background

Fluorescence correlation spectroscopy (FCS) is a highly sensitive method based on analysis of fluctuations in fluorescence intensity to detect and characterize fluorophores in living cells as well as in solution. For instance, FCS allows real-time measurement of two important physical parameters for biochemistry: the average number of molecules in the detection space; and the translational diffusion constant of the molecules through the open volume of detection [1-4].

Cartilage tissue is an avascular tissue, and allows the exchange and transport of nutrients, gases, and metabolites by continuous diffusion instead of through the vasculature [5]. Diffusion in extracellular matrix (ECM) of normal cartilage is thus central to the physiobiological nature of chondrocytes. Cartilage tissue principally consists of ECM and a small number of chondrocytes. The abundant ECM in cartilage is secreted by these chondrocytes. Although ECM provides an environment for the molecular exchanges needed for chondrocyte survival, and plays an important role in physiological activities for the regulation of chondrocyte function, intimate communications between cells and alterations of metabolism, almost no studies have examined the diffusion behaviors of particular molecules from synovial fluid through the ECM of cartilage. Some studies have examined diffusion characteristics and diffusion across articular cartilage using dyes [6,7], glucose [6] and hydrogen [8], To investigate the normal pattern of every different type of molecules in ECM of cartilage, large-scale experiments and varying samples are required. These efforts may help define intricate phenomenon of diffusion in cartiliginous tissue.

Since synovial fluid makes a significant contribution to the nutrition of articular cartilage with direct movement of particular molecules from the synovial space to cartilage by diffusion, understanding the diffusion patterns of molecules from synovial fluid is important. Pathological changes to the ECM cause osteoarthritis (OA), altering not only the physical metabolism of chondrocytes, but also normal molecular exchanges in cartilage.

* Correspondence: sato-m@is.icc.u-tokai.ac.jp
[1]Department of Orthopaedic Surgery, Surgical Science, Tokai University School of Medicine, 143 Shimokasuya, Isehara, Kanagawa 259-1193, Japan
Full list of author information is available at the end of the article

BioMed Central

© 2011 Lee et al; licensee BioMed Central Ltd. This is an Open Access article distributed under the terms of the Creative Commons Attribution License (http://creativecommons.org/licenses/by/2.0), which permits unrestricted use, distribution, and reproduction in any medium, provided the original work is properly cited.

In this study, FCS analysis is made to evaluate albumin movements by means of diffusion in cartilage. Since albumin is the major protein of synovial fluid, tracing albumin protein movements may reveal differences between normal and abnormal states of cartilage.

The purpose of this study was to evaluate the feasibility of FCS for diffusional analysis in normal and chemically degenerated cartilage in relation to albumin, as a representative protein. To select a suitable fluorescent dye before application to cartilage tissue, the physical parameters of several fluorescent dyes were tested and documented. We chose to use a model of degenerated cartilage created by chemical treatment for FCS evaluation, to reflect the denaturation of ECM that might be expected in cartilage tissue during OA.

Results

Degeneration Model of Articular Cartilage

Figure 1 shows the histological appearance of trypsin-treated cartilage samples. As demonstrated by the staining results for porcine articular cartilage using HE, toluidine blue and safranin O, normal cartilage tissue changed into degenerated tissue over time and staining patterns altered after enzyme treatment. At the starting point of enzyme digestion (0 h), cartilage samples showed uniform staining throughout with toluidine blue and safranin O. However, increasing degeneration resulted in larger loss of such staining over time, showing extensive loss of proteogylcans in the tissue.

After 7 h of digestion, no staining was detected in samples using toluidine blue or safranin O, with only HE staining remaining. Therefore, treating cartilage plugs for >7 h was considered to achieve suitable models of degenerated cartilage in these experiments. When 6 h had passed, center regions of digested samples still showed a small portion of intensive staining with safranin O and metachromatic staining with toluidine blue, demonstrating that normal ECM constituents are still present, unlike samples treated for >7 h in which ECM protein components have totally disappeared. Degenerated cartilage and untreated normal cartilage samples were used in FCS measurements.

FCS Measurements

Diffusional behaviors (diffusion coefficient) for all fluorescent dyes utilized in this research were detected by FCS monitoring in PBS solvent. Optimal concentrations of fluorescent dyes differed, which may have resulted from the different chemical, properties of dyes in solusions. The optimal concentrations of Rhodamine 123, Rhodamine 6G, Alexa Fluor 488 hydrazide, and Alexa Fluor 488 conjugated with albumin form bovine serum were, 10^{-7}M, 10^{-7}M, 10^{-8}M, 10^{-5}M, respectively. Two different HA, Artz (MW; 8.0 $\times 10^5$, Seikagaku, Tokyo, Japan) and Suvenly (MW; 2.0 $\times 10^6$, Chugai Pharmaceutical, Tokyo,

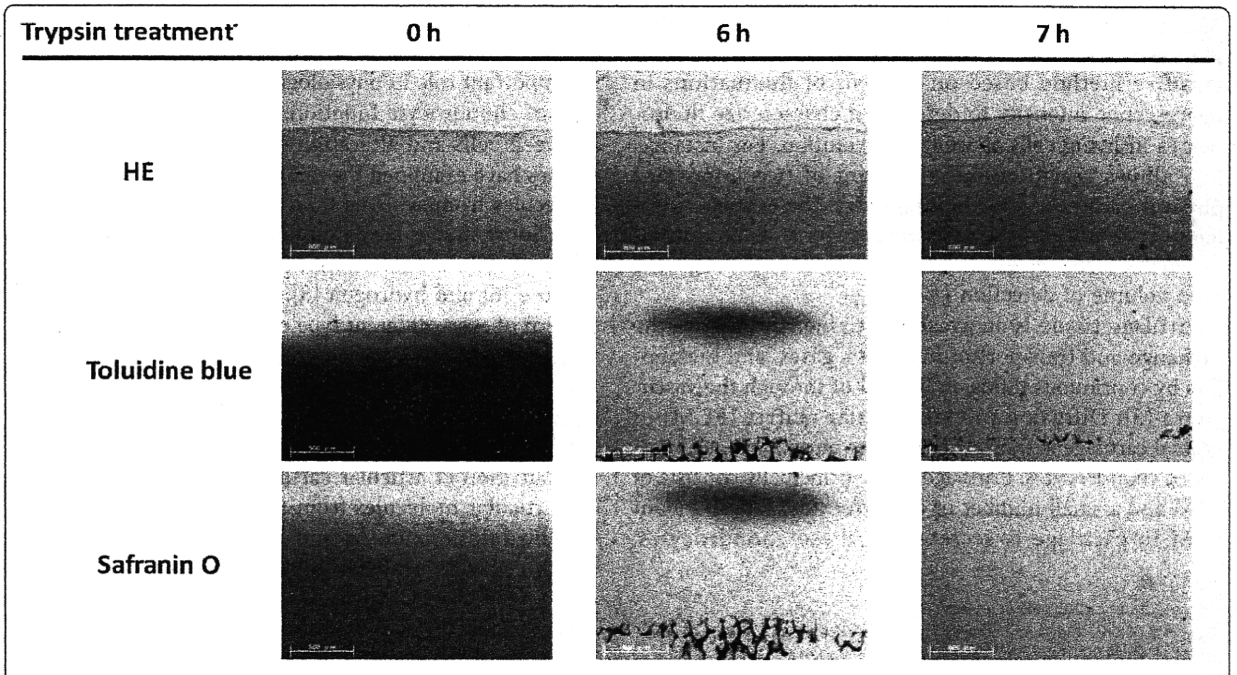

Figure 1 Results of histological examination. After treatment for 7 h, no staining was detected in samples with toluidine blue and safranin O stains, but only HE staining. Therefore, cartilage plugs treated for >7 h were considered as degenerated cartilage models in these experiments. Scale bar = 500 μm.

Japan) were used and their concentrations were 0.1 wt%. Diffusion coefficients of the fluorescent dyes were in the order of PBS > HA (MW, 8.0 $\times 10^5$) > HA (MW, 2.0 $\times 10^6$) (Figure. 2).

Changes of diffusion coefficients are related to the MW of dyes and apparent viscosity of aqueous solution. Fluorescent dyes with a larger MW showed lower diffusion coefficients. At the same time, diffusion coefficients of probe dyes in solution containing HAs decreased with increasing MW of HAs.

The fluorescent dye validated in HAs and cartilage tissues was accepted as a FCS probe, and then applied in the next tests. Since the maximum measurable depth for FCS equipment using Alexa dyes was greater than that using Rhodamine dyes (data not shown), Alexa Fluor 488 was selected as the FCS probe.

FCS measurement tests were performed with Alexa Fluor 488 labled-albumin to trace the diffusion motion of albumin in both normal and degenerated cartilage. FCS data demonstrated an intimate correlation between measureable points (depths from the superficial surface) and enzyme-treatment times (Figure. 3). Increments in these points were correlated with prolongation of trypsin treatment times. FCS data were validated at the range of 120 μm when digestion was conducted for 9 h and >9 h, showing that FCS monitored permeation of the FCS probe at this depth. These focus distances were defined as maximum measurable depths (MMD). When the focus moved over these ranges, no correlation curves were formed, indicating that no movement and no localization of fluorophores is detected in the testing field. As a result of MMD detection, an MMD of 20 μm was chosen for cartilage tissue in the present study.

FCS measurement data for Alexa Fluor 488 conjugated with albumin from bovine serum (Alexa-albumin) as the FCS probe are summarized in Figure 4, which

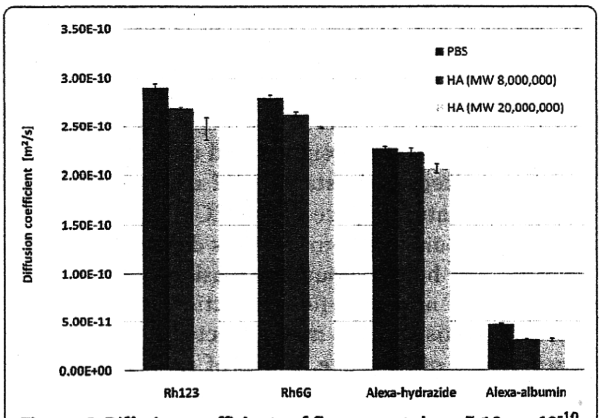

Figure 2 Diffusion coefficients of fluorescent dyes, E-10 = $\times 10^{-10}$. Diffusion coefficients of fluorescent dyes were in the order of PBS > HA (MW, 8.0 $\times 10^5$) > HA (MW, 2.0 $\times 10^6$).

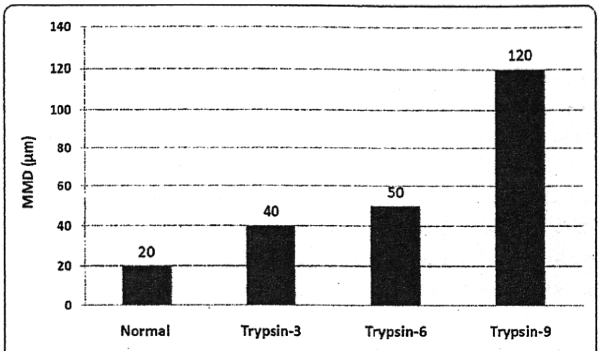

Figure 3 Maximum measurable depth (MMD). FCS data demonstrated an intimate correlation between measureable points, MMD, and prolonging the reaction time of trypsin treatment.

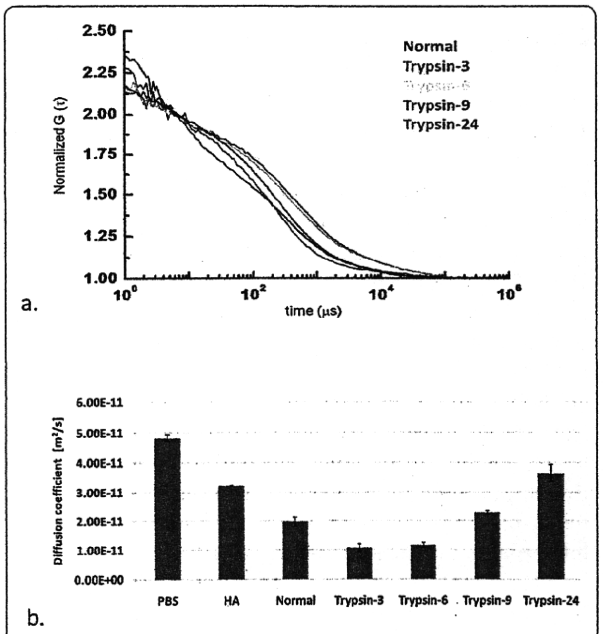

Figure 4 Summary of the FCS measurements. a. Representative of auto correlation curves for Normal, Trypsin-3, Trypsin-6, Trypsin-9, and trypsin-24 b. Diffusion coefficients of Alexa-albumin, E-10 = $\times 10^{-10}$. FCS data demonstrated that diffusion coefficients of Alexa Fluor 488 conjugated with albumin (Alexa-albumin) were greater when measuring degenerated cartilage, indicating that FCS probes moved more freely in degenerated cartilage than in normal tissue. Interestingly, diffusion coefficients for trypsin-3 and trypsin-6 were lower than in normal cartilage. p values of each of groups were under 0.01 which demonstrated the significance of the difference between the groups excluding three of p values between the groups; HA vs.Trypsin-24, Normal vs. Trypsin-9, and Trypsin-3 vs. Trypsin-6. Among these higher values over 0.01, p value between No significant difference was found between Trypsin-3 and Trypsin-6(p = 0.486). Besides, we found a significant difference in the rest of two values which were below 0.05 (p = 0.042; between HA and Trypsin-24, and p = 0.021; Normal and Trypsin-9).

explains the diffusion behaviors of albumin under varying circumstances. We selected one HA with an MW of 8.0×10^5 as representative and performed analyses for this HA. Diffusion coefficients of Alexa-albumin in PBS, HA, trypsin-treated cartilage for 3 h (Trypsin-3), trypsin-treated cartilage for 6 h (Trypsin-6), trypsin-treated cartilage for 9 h (Trypsin-9), and trypsin-treated cartilage for 24 h (Trypsin-24), were 4.83×10^{-11}, 3.23×10^{-11}, 1.06×10^{-11}, 1.15×10^{-11}, 2.30×10^{-11}, and 3.64×10^{-11} m^2/s, respectively. In addition, non-treated normal cartilage was 1.97×10^{-11}, between the ranges of Trypsin-6 and Trypsin-9. An increase in diffusion coefficients was seen with increased duration of chemical digestion.

p values of each of groups were under 0.01 which demonstrated the significance of the difference between the groups excluding three of p values between the groups; HA vs.Trypsin-24, Normal vs. Trypsin-9, and Trypsin-3 vs. Trypsin-6.

Discussion

FCS is an extremely sensitive method for providing concentration and diffusion constant, and molecular interaction of fluorescent molecules in a small volume (femtoliters) of complex mixtures [1-3]. The major sources of fluctuations within the confocal volume are molecular diffusion by Brownian motion, convection, and chemical reactions that change the fluorescence yield. The parameters of molecular dynamics can then be easily extracted by analyzing the time correlation function of fluorescence fluctuations. Information from FCS monitoring is expressed by the autocorrelation curve, then diffusion behaviors are analyzed for comparison. Recent research has been extensively applying FCS measurements to material transportation and interrelationships among biomolecules at the level of the single living cell, and even at the ultra-micro level of intracellular spaces in small organelles [3,9,10].

One important cartilage proteoglycan is HA (comprising glucuronic acid and N-acetyl-glucosamine). This molecule is one of the major components in synovial fluid. HA molecules are also present in cartilage matrix as the backbone structure in proteoglycan aggregates. Since HA plays a major role as an organizer of the ECM [11], we selected HA as a test solution for a FCS probe of cartilage tissue in addition to PBS as a solvent.

In the present study, we tried to measure diffusion properties in cartilage tissues using FCS methods. Before this step, a suitable FCS probe was needed to trace the motion of albumin, and preliminary investigation of several fluorescence dyes was conducted to assess their properties. All diffusion characters of the fluorescent dyes in the present research were detected by FCS equipment in the solvent of PBS and HAs. Since rhodamine dyes showed unstable when applied to cartilage tissue, Alexa dyes utilized as FCS probe. This instability may concern several reasons of character of rhodamine itself such as its strong absorption, tendency to dimerize at higher concentration[12] as so on. Further investigation is needed to determine most proper dye when fluorescent dye is applied to other tissue.

OA is caused by alterations in proteoglycans, degeneration of the collagen network, and an increase in fluid content [13]. Experimental treatments using specific enzymes such as trypsin can simulate these changes [14,15]. In this study, we chose cartilage degeneration created using short-term trypsin treatment as a model of OA. Trypsin treatment of tissue caused a marked loss of proteoglycans in the cartilagenous tissue (Figure. 1). Degenerated cartilage was defined with treatment for >7 h, showing no staining with toluidine blue or safranin O. This result is consistent with previous findings [15].

FCS data demonstrated that diffusion coefficients of Alexa-albumin were greater when measuring degenerated cartilage (Figure. 4), indicating that FCS probes moved more freely in degenerated cartilage than in normal tissue. This phenomenon may occur due to the gradual destruction of ECM structures, finally giving probes a chance to move in a wider space than that in normal cartilage. Diffusion coefficients provide diffusion characteristics of certain molecules. Molecules with larger MW showed lower diffusion coefficients (Figure. 2). Diffusivity decrease with increasing molecular size of flurorescent dyes. Simultaneously, specific molecule described by the diffusion coefficient is affected by the solution environment as shown by tests of HAs showing decreasing diffusion coefficients with increasing MW. Therefore, lower diffusion coefficients indicate difficulties for molecules to diffuse within the surrounding conditions, matching the present results. We were therefore satisfied that the diffusion coefficient for Alexa-albumin can explain the diffusion characteristics in PBS, HAs and cartilage tissue. Interestingly, diffusion coefficients for trypsin-3 and trypsin-6 were lower than in normal cartilage. Considering parameters of diffusion equations and our findings from this study together, this result may be explained as follows. When an aggressive chemically digestion using trypsin induced cartilage degeneration is initiated, early-stage ECM denaturation may change the natural space of the ECM to much more intricate surroundings with exudates digested ECM constituents that hinder albumin diffusion and even have possibility of non-specific interaction with albumin. Moreover, this finding may reflect the time-related degeneration of cartilage, which of early stage differs from that of late stage. Once cartilage has been treated for >6 h, albumin is more diffusible and thus shows an increased diffusion coefficient compared to normal cartilage.

Synovial fluid is a lubricant of intra-articular surfaces and a source of nutrients for hyaline cartilage by diffusion. Synovial protein concentration averages around 42% of the concentration in serum [16]. Among these proteins, albumin constitutes the single largest protein fraction (55-86% of total synovial protein) [16], representing a major contribution to the role of colloid osmotic pressure and other physiobiological functions. As a result, understanding the diffusion characteristics of albumin in such synovial fluid is valuable. Alexa-albumin is made by adding labeled albumin from bovine serum to Alexa-hydrazide. The diffusion behavior of this fluorescent dye was reproducible and simulated experimentally with an *in vitro* model tracing the movement of albumin. Alexa-albumin happened to be commercially available, but FCS probes using other molecules will be also feasible as candidates to create a standard for understanding physiological diffusion in the living body. In addition to albumin as a target molecule for FCS probes, further studies regarding new FCS molecular probes will be essential in the future. The present results reveal that the diffusion state of fluorescence-dyed albumin can be determined by FCS measurement regardless of the intensity of cartilage degeneration.

Some studies have already examined diffusion of particular dyes in cartilage tissue [6-8]. However, methods in those experiments were unsuitable for application as diagnostic tools. These studies needed large volumes of cartilage tissue and were based on macroscopic (gross) experimental data, representing an extremely high level of invasiveness. One of the experiments with dyes and glucose was utilized to evaluate the mechanisms of diffusion across the cartilaginous membrane in a two-compartment device [6]. To diagnosis the pathological alterations in cartilage clinically using diffusion information, simple preparation of samples for examination is critical for achieving minimally invasive diagnosis. In a similar trial in terms of using fluorescence materials and tiny detection fields, Hardingham et al. developed sensitive methods for assessing the matrix assembly around chondrocytes, based on the use of confocal fluorescence recovery after photobleaching (confocal-FRAP) to determine the translational diffusion of fluorescent tracer molecules of defined size [17]. However, this technology was not devised to measure diffusion of particular molecules directly in the ECM, but rather to elucidate the conditions for matrix assembly itself.

More recently, studies have been reported and they showed different methods of measuring diffusion in cartilage using different fluorescence techniques [18-28]. Histological evaluations were conducted on tidemark and calcified cartilage of histological sections with fluorescence agents (fluorecein and rhodamine) [24] itself, and fatty acid labeled with rhodamine fluorescence and albumin[25] using quantitative fluoresce microscopy.

Several researchers reported photobleaching methods pioneered with fluorescence recovery after photobleaching (FLAP) [18,26], fluorescence loss induced by photobleaching (FLIP) [19] and scanning microphotolysis (SCAMP) [20-23]. Fluorecein [18,19], fluorescently-labeled dextran (FITC-conjugated dextran) [20-23] and fluorecein-conjugated bovine serum albumin [26] were utilized as a fluorescent materials to evaluate the diffusivity of human annulus fibrosus [18], calcified cartilage of deep region [19], pericellular matrix of porcine articular cartilage [21], cartilage in normal state [20,23,27,28] or during compression with mechanical stress [22,27,28], ligament [23], growth plate [28] and even agarose [26] and tissue-engineered cartilage [20]. These studies have reported the diffusive transport properties of solutes in both cartilage and collagenous tissue. Some of the experimental results for diffusion coefficients, determined by various methods using fluorescent probes, are summarized in Table 1. According to this table, diffusion coefficient (D) ranged from 2.0×10^{-14} to 290.0×10^{-10} m^2/s. Nonetheless, most of numbers for diffusion coefficients measured with different fluorescent dyes are of similar magnitude to those that measured with FCS in our experiment, on the order of 10^{-11} to 10^{-10}. Our adaptation of the FCS technique can be used to measure site-specific diffusivity in an extremely small detection volume of tissue. The diffusion coefficients measured with Alexa-albumin in the normal cartilage (1.97×10^{-11} m^2/s) and degenerated cartilage (1.06×10^{-11}, 1.15×10^{-11}, 2.30×10^{-11}, and 3.64×10^{-11} m^2/s), are in good agreement with values of the order measured previously using other techniques (3.1×10^{-11} m^2/s using fluorescence recovery after photobleaching and 4.0×10^{-11} m^2/s using radiotracertracking [21]. Among these previous studies with tagged with albumin probes [25,26], the diffusion coefficients in cartilage ranged from 0.3×10^{-11} to 29.0×10^{-11} m^2/s (Table 1). Considering the range of methods and possible variation in the properties of various cartilage sources, present results (Figure. 4) are in reasonable agreement with these data, supporting the accuracy of our methods. Advantages of our methods include quickness of diffusion measurements, simplicity, noninvasiveness, and the ability to quantify the molecular diffusion in the different individual tissues.

The apparently wide range of diffusivities of normal cartilage and degenerated cartilage highlights the influence of physical properties of both the fluorescent molecule and the ECM on hindered transport within biological systems. This may results from the circumstantial and collateral conditions such as tissue conditions (animal species, type of cartilage, preservation until measurement, compression etc.), solutions utilized

Table 1 Summary of experimental results for diffusion coefficient, *D*, from recent studies using fluorescent dye

Fluorescent dye	Method	Specimen	Temp. (°C)	D ($\times 10^{-10} m^2/s$)	Ref.
Fluorecein (332 Da)	Fluorescence recovery after photobleaching (FRAP)	Human intervertebral discs	22	0.38 ± 0.25 ~ 2.68 ± 0.84	[18]
		Inner, middle and outer regions of annulus fibrosus			
Fluorecein (376 Da)	Fluorescence loss induced by photobleaching (FLIP).	Murine (C57BL6J) distal humurs	4		[19]
		Subchondral bone		0.0002 ~ 0.012 (0.0007 ± 0.0003)	
		Calcified cartilage		0.0005 ~ 0.009 (0.0026 ± 0.0022)	
Fluorescein isothiocyante (FITC)-tagged dextran (3, 40, 70, and 500 kDa)	Fluorescence recovery after photobleaching (FRAP)	Tissue engineered cartilage from human adipose-derived stem cell with or without scaffold (alginate, agarose, fibrin and gelatin)	37	0.16 ± 0.08 (Day 28, cultured within fibrin in control media using 500 kDa)	[20]
			or	~ 18.10 ± 3.94 (Day 1, cultured within gelatine in chondrogenic media using 3 kDa)	
			?		
Fluorescein isothiocyante (FITC)-tagged dextran (70 kDa)	Scanning microphotolysis (SCAMP).	Porcine femoral condyle	?		[21]
		Healthy cartilage			
		Extracellular matrix		0.23 ± 0.02	
		Pericellular matrix		0.19 ± 0.02	
		Osteoarthritic cartilage			
		Extracellular matrix		0.23 ± 0.02	
		Pericellular matrix		0.23 ± 0.02	
Fluorescein isothiocyante (FITC)-tagged dextran (70 kDa)	Scanning microphotolysis (SCAMP) and Fluorescence imaging of continuous point photobleaching (FICOPP)	Porcine femoral condyle	?		[22]
		Normal cartilage		0.33	
		Compressed cartilage		0.07	
Fluorescein isothiocyante (FITC)-tagged dextran (3 and 500 kDa)	Fluorescence imaging of continuous point photobleaching (FICOPP)	Collagenous tissues	4	Inexpressible because authors explain diffusivity by not diffusion coefficient but by diffusivity ratio for comparisons	[23]
		3% agarose gel	or		
		Lateral collateral ligaments (Porcine)	?		
Rhodamine B (443 Da, cationic), Rhodamine B (479 Da, neutral but polar), Fluorecein (332 Da), and Na-fluorecein (376 Da)	Quantitative fluorescence microscopy on histological sections	Equine forelimb	4	0.0098 ± 0.0013 ~ 0.037 ± 0.003	[24]
		Subchondral bone			
		Calcified cartilage			
Bovine serum albumin labeled with rhodamine - maleimide and Nitrobenz -2-oxa-1,3-diazole (NBD) -labelled lauric acid (378 Da) bound to the fluorescent albumin	Quantitative fluorescence microscopy on histological sections	Equine metacarpal-phalangeal joints	4	9.0 ± 2.0 (48 h-incubation, using albumin)	[25]
				~	
				290.0 ± 10.0 (2 h-incubation, using lauric acid)	

Table 1 Summary of experimental results for diffusion coefficient, *D*, from recent studies using fluorescent dye *(Continued)*

Fluorescein-conjugated bovine serum albumin (66 kDa).	Fluorescence recovery after photobleaching (FRAP)	3~8% agarose gel	24	0.164 ± 0.018 ~ 0.411 ± 0.008	[26]
		Porcine growth plate		0.0387 ~ 0.4922	
Tetramethylrhodamine (TMR) -tagged dextran (3,10, and 40 kDa) and tetramethylrhodamine (430 Da) itself,	Novel experimental apparatus and desorption fluorescence method.	Bovine femurs	4	0.19 ± 0.02 (8% compression, using 40 kDa dextran)	[27,28]
		Compressed cartilage		~ 0.52 ± 0.06 (8% compression, using 430 Da TMR)	

For studies investigating anisotropic diffusivity, the smallest to the largest value of the diffusion coefficient is reported. (Temp.: Temperature, Ref.: Reference).

(ingredient, ion contents, buffer, culture media, manufacturing company etc.), tissue processing (treatment and incubation time, condition, time, temperature etc.), and properties of each fluorescent dye (shape, molecular weight, physical properties electric charge, the hydrophilic or hydrophobic natures, manufacturing company ect).

Diffusion coefficients can also be measured by fluorescence recovery after photobleaching (FRAP). However, most of these methods to analyze FRAP data expect the homogeneity in the measurable field of the bleached area and fail to assume geometrical restrictions to diffusion. Accordingly, diffusion coefficients in inhomogeneous materials, such as most biological tissues, cannot be evaluated correctly.

Several methods are available to analyze FRAP data, each with its own characteristics [29]. The technique to apply depends on the data which are aimed for and the tissue that is being probed. Presumably the most adaptable tool currently utilized is by spatial Fourier analysis of a sequence of FRAP images [30]. With this method, anisotropic diffusion, flow, matrix binding, and diffusivity in multiple components of a gel can be evaluated, whereas the evaluation is independent on the geometry of the bleached area [26]. This limitation originates from the requirement that the boundary of the image must have a constant intensity value. In practice, this means that a large area, relative to the bleached area, is to be imaged. This decreases the amount of signal in the images. The same requirement of constant boundary intensity applies to this method [26]. The average intensity of the images is allowed to change during the measurements. In practice, this means that the bleached area typically constitutes a large part of the acquired images to enhance the signal. Note that the lower limit to the physical size of the bleached area is defined by the point-spread function. This needs to be considered if small bleached areas are used [26].

Compared with photobleaching methods, FCS need minimum excitation power. Hence, this technique requires lower power and much small amount of fluorescent dyes to get information of FCS data. It is not easy to calculate directly the diffusion coefficient with photobleaching tools, however, we can promptly get the absolute value of diffusion coefficient with FCS instrument. One of the merits using FCS is that various concentrations of the fluorescent molecules used are easily monitored. It is worth considering the complementary use of FCS and photobleaching methods with their different characteristics.

To the best of our knowledge, no previous studies have demonstrated the feasibility of FCS for direct measurement of diffusional behaviors of fluorescently labeled albumin in the ECM of cartilage tissue, and this approach may represent a potential and useful evaluation tool. If diffusion in the ECM can be clarified and categorized with this new method by standardization of FCS data under various cartilage conditions, FCS will be applicable for the early diagnosis of OA, which is accompanied by increased destruction of ECM elements, and also as a tool for evaluating bio-engineered artificial cartilage for autologous chondrocyte implantation. Besides changes in diffusion characteristics of molecules in the cartilage ECM, additional and complementary information can be adopted to clarify the clinical picture. For example, alterations in the ECM simultaneously induce changes in viscoelasticity of the cartilage. Monitoring changes in viscoelasticity is possible using reliable techniques such as photoacoustic measurement [15,31,32]. Such information could be used together with diffusion characteristics to evaluate optimal conditions for ECM and to test bioengineered neocartilage constructs, and will suggest new criteria for real-time evaluation with small quantities of samples under minimally invasive arthroscopic surgery with FCS analysis system.

Conclusions

This work offers the first demonstration of the capabilities of FCS for direct measurement of diffusion behaviors of ECM in cartilage. This sensitive measurement

technique provides great advantages in detecting diffusible molecules due to the ability to achieve rapid measurements from small sample volumes.

Methods

Sample Preparation

Fresh swine knees (n = 5) were obtained from a local slaughterhouse at Kanagawa meat center (Frieden, Kanagawa, Japan). Cartilage tissue from the femur was prepared within 4 h as follows. The cartilage tissues of delivered knee joints were cut out into cylindrical cartilage plugs (diameter, 5 mm; depth, 1 mm; n = 240) using a biopsy punch (Kai Industries, Seki City, Japan) and disposable scalpels (Akiyama, Tokyo, Japan). Porcine cartilage specimens were initially incubated under physiological conditions (37°C, 5% CO_2) in physiological saline (Otsuka Pharmaceutical Factory, Tokushima, Japan) until the next procedure.

Degenerated Cartilage Models

Addition of enzymes was used for experimental degradation of the tissue matrix using phosphate-buffered saline (PBS) (Wako Pure Chemical, Osaka, Japan) containing 0.1% trypsin solution (1 mg/ml; Invitrogen, Carlsbad, CA, USA) to degrade primarily proteoglycans. The trypsin treatment time was minimally 1 h and varied up to 24 h every hour to control the extent of degeneration.

To stop the trypsin reaction, an equal volume of fetal bovine serum (FBS) (Invitrogen) was added and then incubated for a further 30 min. The digested cartilage samples were thoroughly rinsed with PBS to remove residual trypsin and FBS.

Chemically treated and non-treated cartilage discs were then divided for histopathological assessment and FCS measurement. To perform the histopathological assessment, samples were fixed in 4% paraformaldehyde and embedded in paraffin, and 4-mm-thick sections were prepared. Histological staining was performed using hematoxylin and eosin (HE), toluidine blue and safranin O to visualize the degree of ECM degeneration within specimens. Samples for FSC were prepared and used for FCS measurements with the FCS probes as described below.

Preparation and Selection of Fluorescent Dye

To determine properly applicable fluorescent dyes (FCS probes) for cartilage tissue, commercially available fluorescent dyes were obtained, including Rhodamine 123 (Rh123) (molecular weight (MW), 380.82; Sigma-Aldrich, St. Louis, MO) Rhodamine 6G (Rh6G) (MW, 479.01; Sigma-Aldrich), Alexa Fluor 488 hydrazide (Alexa-hydrazide) (MW, 570.48; Molecular Probes, Eugene, OR). First, optimal concentrations of the fluorescent dyes in PBS (100 μl) were measured and analyzed, then applicable concentrations of each dye solution (100 μl) were mixed with 100 μl of hyaluronic acid sodium (HA) and tested.

To optimalize the concentrations of these fluorescent probes, FCS measurement were conducted with ten-fold serial dilutions of each fluorescent agents adding PBS. After receiving the FCS data from these measurements, the calculatable data of each concentration of dyes were obtained by expressing autocorrelation curve.

Two different molecular sizes of HA with average MWs of 8.0 $\times 10^5$ (Artz; Seikagaku, Tokyo, Japan) and 2.00 $\times 10^6$ (Suvenly; Chugai Pharmaceutical, Tokyo, Japan) were used in this experiment.

In addition to these measurements, albumin-conjugated fluorescent dyes were adopted to evaluate the diffusion behavior of albumin protein. Alexa Fluor 488 conjugated with albumin from bovine serum (Alexa-albumin) (MW approximately 66,000; Molecular Probes) was tested and analyzed with PBS, two differ types of HA solutions and cartilage samples. Physiological parameters affecting the diffusion behaviors of fluorescence dyes were measured and monitored with FSC measurement, including counts per molecule, count rate, diffusion time, particle number, correlation, structure parameter, triplet fraction and triplet time. In the case of measurement within cartilage tissues, length from the superficial surface to the maximum measureable points was experimentally determined.

Statistical Analysis

All results of the experiments are expressed as the means ± SE. The mean values for each group were compared by ANOVA and then by using Fisher's least significant difference method. Values of $p < 0.05$ were considered the minimum level of statistical significance

FCS Measurement and Analysis

FCS was performed using an LSM510-ConfoCor 2 system (Carl Zeiss, Oberkochen, Germany), as described elsewhere [33,34]. FCS measurements of all samples were recorded at 25°C.

Various concentrations of the candidate fluorescent dyes were incubated with purified PBS at 37°C in an atmosphere of 5% CO_2 and 95% air over 30 min. Aliquots (100 μl) were arrayed onto Lab-Tek chambered cover-glass (Nalge Nunc International, Naperville, IL, USA) with eight wells and <140-μm-thick cover-glass on the bottom. Cartilage specimens were placed on Lab-Tek chambered cover-glass with eight wells and 100 μl of FCS probe-solution was applied over the samples.

Each acquired correlation data set was analyzed by software supplied by Carl Zeiss with a fitting program (FCS Access Fit software; EVOTEC BioSystems, Hamburg, Germany), or exported to Igor Pro software (IGOR Pro 5.05a; Wavemetrics, Lake Oswego, OR). In the FCS analysis, the diffusion coefficient is represented by the average of five FCS measurements

The autocorrelation curve is obtained by correlating the fluorescence intensity trace shifting within a time interval. The time shift τ is varied, and the correlation curve is obtained by multiplying the deviation of the average intensity, δF, at the time point t with the deviation at time point $t + \tau$ and averaging over the whole trace. Finally, the correlation function, $G(\tau)$, is normalized with the squared average signal.

$$G(\tau) = \frac{\langle \delta F(t) \delta F(t+\tau) \rangle}{\langle F \rangle^2} \quad (1)$$

Further practical considerations in the calculation of FCS curves from a fluorescence intensity trace are detailed elsewhere [35-37].

Diffusion of one single component is commonly fitted with the standard model [38]:

$$G(\tau) = 1 + \frac{1}{N}\left(1 + \frac{4D\tau}{\omega_0^2}\right)^{-1}\left(1 + \frac{4D\tau}{z_0^2}\right)^{-\frac{1}{2}} \quad (2)$$

The resulting ideal probe volume is approximated by a Gaussian profile with the extension ω_0 in x and y directions and z_0 in the z direction [39]. N is the number of fluorescence molecules in the detection volume, defined by a radius ω_0 and a length 2 z_0. The diffusion time (τ_D) is related to the traditional diffusion constant of the diffusion coefficient D. As this time corresponds to Equation 3, the diffusion coefficient D is obtained:

$$\tau_D = \frac{\omega_0^2}{4D} \quad (3)$$

The diffusion of spherical molecules is related to various physical parameters by the Stokes-Einstain equation as follows:

$$D = \frac{k_B T}{6\pi\eta r} \quad (4)$$

where T is the absolute temperature, r is the radius of the spherical molecule, η is the fluid-phase viscosity of the solvent, and k_B is the Boltzman constant.

When measuring the diffusion time of samples (τ_{sample}) and rhodamine 6G (τ_{Rh6G}) with the FSC system, the diffusion coefficient of rhodamine 6G at 20°C [40], 2.8 $\times 10^{-10}$ m^2/s, was used as an authentic value for determination of the diffusion coefficient of samples (D_{sample}) measured on the expectation of a proportional relationship based on the following equation:

$$\frac{D_{sample}}{D_{Rh6G}} = \frac{\tau_{Rh6G}}{\tau_{sample}} \quad (5)$$

Acknowledgements
The authors thank Dr. Chan-Gi Pack (Cellular Systems Modeling Team, RIKEN Advanced Science Institute, Japan) for the critical review and comments on the manuscript.

Author details
[1]Department of Orthopaedic Surgery, Surgical Science, Tokai University School of Medicine, 143 Shimokasuya, Isehara, Kanagawa 259-1193, Japan. [2]Department of Biomedical Science & Technology, Institute of Biomedical Science & Technology (IBST), Konkuk University, 1 Hwayang-dong, Gwangjin-gu, Seoul 143-701, Korea. [3]Eco-Soft Materials Research Unit, RIKEN (The Institute of Physical and Chemical Research), 2-1 Hirosawa, Wako, Saitama 351-0198, Japan.

Authors' contributions
JIL and KU performed the research. JIL, KU and MS analyzed the data. JIL took charge of the statistical analyses. JIL, KU, MS, and JM wrote the manuscript. All authors have read and approved the final manuscript.

Competing interests
The authors declare that they have no competing interests.

Received: 15 June 2010 Accepted: 2 March 2011
Published: 2 March 2011

References

1. Aragon SR, Pecora R: **Fluorescence correlation spectroscopy as a probe of molecular dynamics.** *J Chem Phys* 1976, 64:1791-1803.
2. Elson EL, Magde D: **Fluorescence correlation spectroscopy. I. Conceptual basis and theory.** *Biopolymers* 1974, 13(1):1-27.
3. Thompson NL: **Fluorescence correlation spectroscopy.** *Topics in fluorescence spectroscopy* 1991, 1:337-378.
4. Pack C, Saito K, Tamura M, Kinjo M: **Microenvironment and effect of energy depletion in the nucleus analyzed by mobility of multiple oligomeric EGFPs.** *Biophys J* 2006, 91(10):3921-3936.
5. Ge Z, Hu Y, Heng BC, Yang Z, Ouyang H, Lee EH, Cao T: **Osteoarthritis and therapy.** *Arthritis and rheumatism* 2006, 55(3):493-500.
6. Maroudas A, Bullough P, Swanson SA, Freeman MA: **The permeability of articular cartilage.** *J Bone Joint Surg Br* 1968, 50(1):166-177.
7. Brower T, Akahoshi Y, Orlic P: **The diffusion of dyes through articular cartilage in vivo.** *J Bone Joint Surg Am* 1962, 44(3):456.
8. Ogata K, Whiteside LA, Lesker PA: **Subchondral route for nutrition to articular cartilage in the rabbit. Measurement of diffusion with hydrogen gas in vivo.** *J Bone Joint Surg Am* 1978, 60(7):905-910.
9. Bulseco DA, Wolf DE: **Fluorescence correlation spectroscopy: molecular complexing in solution and in living cells.** *Methods Cell Biol* 2007, 81:525-559.
10. Schwille P, Haupts U, Maiti S, Webb WW: **Molecular dynamics in living cells observed by fluorescence correlation spectroscopy with one- and two-photon excitation.** *Biophys J* 1999, 77(4):2251-2265.
11. Suh JK, Matthew HW: **Application of chitosan-based polysaccharide biomaterials in cartilage tissue engineering: a review.** *Biomaterials* 2000, 21(24):2589-2598.
12. Qiu Y, Zhang F, Zhao F, Tang Y, Song X: **Degradation of rhodamine 6G in the peroxyoxalate chemiluminescent reaction.** *Journal of Photochemistry and Photobiology A: Chemistry* 1995, 85(3):281-284.
13. Suh JK, Youn I, Fu FH: **An in situ calibration of an ultrasound transducer: a potential application for an ultrasonic indentation test of articular cartilage.** *J Biomech* 2001, 34(10):1347-1353.

14. Lyyra T, Arokoski JPA, Oksala N, Vihko A, Hyttinen M, Jurvelin JS, Kiviranta I: **Experimental validation of arthroscopic cartilage stiffness measurement using enzymatically degraded cartilage samples.** *Physics in Medicine and Biology* 1999, **44**:525-536.
15. Ishihara M, Sato M, Kaneshiro N, Mitani G, Sato S, Mochida J, Kikuchi M: **Development of a diagnostic system for osteoarthritis using a photoacoustic measurement method.** *Lasers Surg Med* 2006, **38**(3):249-255.
16. Knox P, Levick JR, McDonald JN: **Synovial fluid–its mass, macromolecular content and pressure in major limb joints of the rabbit.** *Q J Exp Physiol* 1988, **73**(1):33-45.
17. Hardingham T, Tew S, Murdoch A: **Tissue engineering: chondrocytes and cartilage.** *Arthritis Res* 2002, **4**(Suppl 3):S63-68.
18. Travascio F, Jackson AR, Brown MD, Gu WY: **Relationship between solute transport properties and tissue morphology in human annulus fibrosus.** *J Orthop Res* 2009, **27**(12):1625-1630.
19. Pan J, Zhou X, Li W, Novotny JE, Doty SB, Wang L: **In situ measurement of transport between subchondral bone and articular cartilage.** *J Orthop Res* 2009, **27**(10):1347-1352.
20. Leddy HA, Awad HA, Guilak F: **Molecular diffusion in tissue-engineered cartilage constructs: effects of scaffold material, time, and culture conditions.** *J Biomed Mater Res B Appl Biomater* 2004, **70**(2):397-406.
21. Leddy HA, Christensen SE, Guilak F: **Microscale diffusion properties of the cartilage pericellular matrix measured using 3D scanning microphotolysis.** *J Biomech Eng* 2008, **130**(6):061002.
22. Leddy HA, Guilak F: **Site-specific effects of compression on macromolecular diffusion in articular cartilage.** *Biophys J* 2008, **95**(10):4890-4895.
23. Leddy HA, Haider MA, Guilak F: **Diffusional anisotropy in collagenous tissues: fluorescence imaging of continuous point photobleaching.** *Biophys J* 2006, **91**(1):311-316.
24. Arkill KP, Winlove CP: **Solute transport in the deep and calcified zones of articular cartilage.** *Osteoarthritis Cartilage* 2008, **16**(6):708-714.
25. Arkill KP, Winlove CP: **Fatty acid transport in articular cartilage.** *Arch Biochem Biophys* 2006, **456**(1):71-78.
26. Sniekers YH, van Donkelaar CC: **Determining diffusion coefficients in inhomogeneous tissues using fluorescence recovery after photobleaching.** *Biophys J* 2005, **89**(2):1302-1307.
27. Quinn TM, Kocian P, Meister JJ: **Static compression is associated with decreased diffusivity of dextrans in cartilage explants.** *Arch Biochem Biophys* 2000, **384**(2):327-334.
28. Quinn TM, Morel V, Meister JJ: **Static compression of articular cartilage can reduce solute diffusivity and partitioning: implications for the chondrocyte biological response.** *J Biomech* 2001, **34**(11):1463-1469.
29. Carrero G, McDonald D, Crawford E, de Vries G, Hendzel MJ: **Using FRAP and mathematical modeling to determine the in vivo kinetics of nuclear proteins.** *Methods* 2003, **29**(1):14-28.
30. Berk DA, Yuan F, Leunig M, Jain RK: **Fluorescence photobleaching with spatial Fourier analysis: measurement of diffusion in light-scattering media.** *Biophys J* 1993, **65**(6):2428-2436.
31. Ishihara M, Sato M, Sato S, Kikuchi T, Mochida J, Kikuchi M: **Usefulness of photoacoustic measurements for evaluation of biomechanical properties of tissue-engineered cartilage.** *Tissue engineering* 2005, **11**(7-8):1234-1243.
32. Kutsuna T, Sato M, Ishihara M, Furukawa KS, Nagai T, Kikuchi M, Ushida T, Mochida J: **Noninvasive evaluation of tissue-engineered cartilage with time-resolved laser-induced fluorescence spectroscopy.** *Tissue Eng Part C Methods* 2010, **16**(3):365-373.
33. Pack CG, Nishimura G, Tamura M, Aoki K, Taguchi H, Yoshida M, Kinjo M: **Analysis of interaction between chaperonin GroEL and its substrate using fluorescence correlation spectroscopy.** *Cytometry* 1999, **36**(3):247-253.
34. Kinjo M: **Detection of asymmetric PCR products in homogeneous solution by fluorescence correlation spectroscopy.** *Biotechniques* 1998, **25**(4):706-712, 714-705.
35. Grunwald D, Cardoso MC, Leonhardt H, Buschmann V: **Diffusion and binding properties investigated by Fluorescence Correlation Spectroscopy (FCS).** *Curr Pharm Biotechnol* 2005, **6**(5):381-386.
36. Wahl M, Gregor I, Patting M, Enderlein J: **Fast calculation of fluorescence correlation data with asynchronous time-correlated single-photon counting.** *Opt Express* 2003, **11**(26):3583-3591.
37. Xiao Y, Buschmann V, Weston KD: **Scanning fluorescence correlation spectroscopy: a tool for probing microsecond dynamics of surface-bound fluorescent species.** *Anal Chem* 2005, **77**(1):36-46.
38. Rigler R, Mets , Widengren J, Kask P: **Fluorescence correlation spectroscopy with high count rate and low background: analysis of translational diffusion.** *European Biophysics Journal* 1993, **22**(3):169-175.
39. Marrocco M: **Fluorescence correlation spectroscopy: incorporation of probe volume effects into the three-dimensional Gaussian approximation.** *Appl Opt* 2004, **43**(27):5251-5262.
40. Magde D, Elson EL, Webb WW: **Fluorescence correlation spectroscopy. II. An experimental realization.** *Biopolymers* 1974, **13**(1):29-61.

doi:10.1186/1472-6750-11-19
Cite this article as: Lee *et al.*: Measurement of diffusion in articular cartilage using fluorescence correlation spectroscopy. *BMC Biotechnology* 2011 11:19.

Submit your next manuscript to BioMed Central and take full advantage of:

- Convenient online submission
- Thorough peer review
- No space constraints or color figure charges
- Immediate publication on acceptance
- Inclusion in PubMed, CAS, Scopus and Google Scholar
- Research which is freely available for redistribution

Submit your manuscript at
www.biomedcentral.com/submit

BioMed Central

関節軟骨損傷修復のための軟骨細胞シート

佐藤正人* 三谷玄弥 伊藤聡
鵜養拓 小久保舞美 持田譲治

背景

われわれは，これまでに関節軟骨の修復·再生に関して，基礎的研究を主に *in vivo* 実験で確認してきた。例えば，組織工学的手法による軟骨再生に適した担体作製に関する研究[1]，至適細胞外環境の構築に関する研究[2)~5)]，同種の組織工学的軟骨，線維輪移植による組織修復·再生に関する研究[6)~9)]，ならびに軟骨細胞シート移植による軟骨修復·再生に関する研究[10)11)14)~16)]などである。これら一連の研究により，軟骨の修復·再生におけるホスト（レシピエント）由来細胞とドナー由来細胞との相互作用の重要性を確認した。そして，組織修復·再生に必要最小限のイニシエーター（組織工学的軟骨）があれば，ホスト由来細胞が主導的に組織修復を促進することを見いだした[6)13)14)]。

温度応答性培養皿による軟骨細胞シート

温度応答性培養皿は，東京女子医科大学岡野光夫教授が開発したもので，独自のナノ表面設計により温度応答性ポリマー（PIPAAm）を器材表面に固定化することで器材表面は32℃を境に可逆的に疎水性（細胞接着表面）親水性（細胞遊離表面）に変化する。この特性により，トリプシン等，細胞に損傷を与える酵素を一切用いることなく，温度を20~25℃にして10~30分程度待つだけで，無傷な細胞と細胞外マトリックスがシート状に回収可能である。温度応答性培養皿で作製した積層化軟骨細胞シートは，通常の培養皿で得られる培養細胞とは異なる特性を有し，これらを利用した関節軟骨修復再生効果をわれわれは初めて報告し[10)]，組織修復能力に優れた積層化軟骨細胞シートの特性を明らかにした[11)15)16)]（**図1**）。

*Masato SATO，東海大学医学部，外科学系整形外科学

軟骨細胞シートによる関節治療の可能性

軟骨細胞シートは力学的には脆弱ではあるが，優れた接着性を有し，損傷した軟骨からのプロテオグリカンの流出を阻止し，関節液中のカタボリックファクターから軟骨を保護し，成長因子の持続的な供給源であると共に，さらに骨髄由来幹細胞の軟骨分化を促進するイニシエーターとしても機能しており，単なる軟骨再生というよりは，むしろ自己修復能力を向上させる効果により，軟骨は修復·再生されている。つまり，変形性関節症において常に混在しながら存在する軟骨全層欠損（軟骨下骨まで達する骨軟骨損傷で，従来の再生医療のターゲット＝**図2A**）と軟骨部分損傷（**図2B**）の両タイプの軟骨損傷に対して，細胞シートによる修復·再生効果を確認し，細胞シート工学という日本発のオリジナルな技術により，変形性関節症の治療にまで踏み込んだ再生医療の実現を目指している。

文献

1) Sato M et al：An atelocollagen honeycomb-shaped scaffold with a membrane seal (ACHMS-scaffold) for the culture of annulus fibrosus cells from an intervertebral disc. J Biomed Mater Res Part A **64**：249-256, 2003
2) Ishihara M et al：Photocrosslinkable chitosan as a dressing for wound occlusion and accelerator in healing process. Biomaterials **23**：833-840, 2002
3) Ishihara M et al：Heparin-carrying polystyrene (HCPS)-bound c. lagen substratum to immobilize heparin-binding growth factors and to enhance cellular growth. J Biomed Mater Res **56**：536-544, 2001
4) Ono K et al：Experiment, evaluation of photocrosslinkable chitosan as a biologic adhesive with surgical applications. Surgery **130**：844-850, 2001
5) Ishihara M et al：Acceleration of wound contraction and healing with a photocrosslinkable chitosan hydrogel. Wound Repair Regen **9**：513-521, 2001
6) Masuoka K et al：Tissue engineering of articular cartilage using an allograft of cultured chondrocytes in a membrane-sealed atelocollagen honeycomb-shaped scaffold (ACHMS scaffold). J Biomed Mater Res Part B Appl Biomater **75**：177-184, 2005
7) Sato M et al：Effects of growth factors on heparin-carrying polystyrene-coated atelocollagen scaffold for articular cartilage tissue engineering. J Biomed Mater Res Part B Appl Biomater **83**：181-188, 2007
8) Sato M et al：An experimental study of the regenera-